Supplementary Electronic Information (ESI)

Potent Mannose-Modified Pillararene-BODIPY System for Photodynamic Therapy

Pitiphoom Sangiamkittikul,[a] Sopon Nuchpun,[b] Kanlaya Prapainop Katewongsa,[b] Tawinan Cheiwchanchamnangij,[c] Korawit Khamphaijun,[a] Thanthapatra Bunchuay,[a] Nattapon Panupinthu,[d,e] Worakrit Saiyasombat,[f] Sitthivut Charoensutthivarakul,[g] Supavadee Kiatisevi[a]*

[a] Department of Chemistry and Center of Excellence for Innovation in Chemistry (PERCH-CIC), Faculty of Science, Mahidol University, Bangkok, Thailand
[b] Department of Biochemistry, Faculty of Science, Mahidol University, Bangkok, Thailand
[c] Department of Physics, Faculty of Science, Mahidol University, Bangkok, Thailand
[d] Center of Calcium and Bone Research (COCAB), Faculty of Science, Mahidol University, Bangkok, Thailand
[e] Department of Physiology, Faculty of Science, Mahidol University, Bangkok, Thailand
[f] Institute of Nutrition, Mahidol University, Nakhon Pathom, Thailand
[g] School of Bioinnovation and Bio-Based Product Intelligence, Faculty of Science, Mahidol University, Bangkok, Thailand

*Corresponding author: Supavadee Kiatisevi, E-mail address: supavadee.mon@mahidol.ac.th

Supplementary Electronic Information (ESI)

Table of Contents

Supplementary Electronic Information (ESI)

List of Schemes

List of Figures

Supplementary Electronic Information (ESI)

1. Synthesis of PS3 and WP5

1.1 Synthesis of PS3

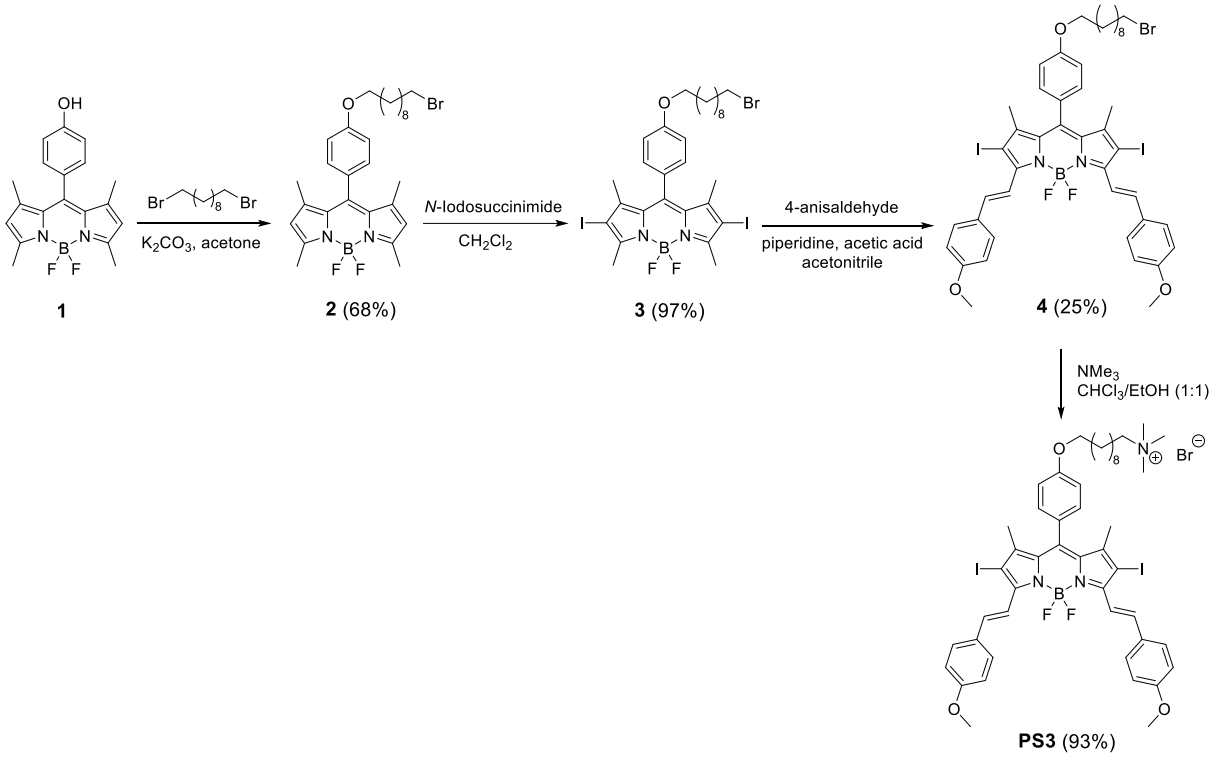

Scheme S1. Synthesis of **PS3**.

*1.1.1 Synthesis of 8-(4-hydroxyphenyl)-1,3,5,7-tetramethyl-4,4-difluoro-4-bora-3a,4a-diaza-s-indacene (**1**)*

Compound **1** was prepared according to the literature.[1,2] In a 2-neck round bottom flask, 4-hydroxy benzaldehyde (0.360 g, 2.9 mmol) and 2,4-dimethylpyrrole (0.7 mL, 6.8 mmol) were mixed in dry THF (80 mL). TFA (0.1 ml, 1.3 mmol) was then added and stirred under argon for 18 h. DDQ (0.734 mg, 3.2 mmol) in 80 mL THF was added dropwise. The reaction mixture was stirred for 4 h at room temperature and was cooled in an ice bath. Triethylamine (5 mL, 35.9 mmol) was added, and the mixture was stirred for 30 min. $BF_3 \cdot OEt_2$ (5 mL, 40.5 mmol) was then added, and the resulting mixture was stirred at room temperature for 18 h. THF was removed under reduced pressure, and the crude product was dissolved in CH_2Cl_2. The solution was washed sequentially with brine, saturated $NaHCO_3$ solution, and water. The organic phase was dried over Na_2SO_4 and evaporated to dryness. The residue was purified by column chromatography on silica gel with 1:2 CH_2Cl_2/hexane to obtain **1** as a red solid (550 mg, 1.61 mmol, 55%). **^{1}H-NMR** (400 MHz, $CDCl_3$, ppm): δ = 7.11 (d, J = 8.5 Hz, 2H; $CH_{aromatic}$), 6.94 (d, J = 8.5 Hz, 2H; $CH_{aromatic}$), 5.97 (s, 2H; CH), 2.55 (s, 6H; CH_3), 1.44 (s, 6H; CH_3). **^{13}C-NMR**

(100 MHz, $CDCl_3$, ppm): δ=156.8, 155.8, 143.7, 142.2 132.2, 129.8, 127.6, 121.6, 116.6, 15.0. **DART-HRMS** (ESI) *m/z*: calcd. for $C_{19}H_{20}BF_2N_2O^+$ $[M+H]^+$, 341.1631; found, 341.1637.

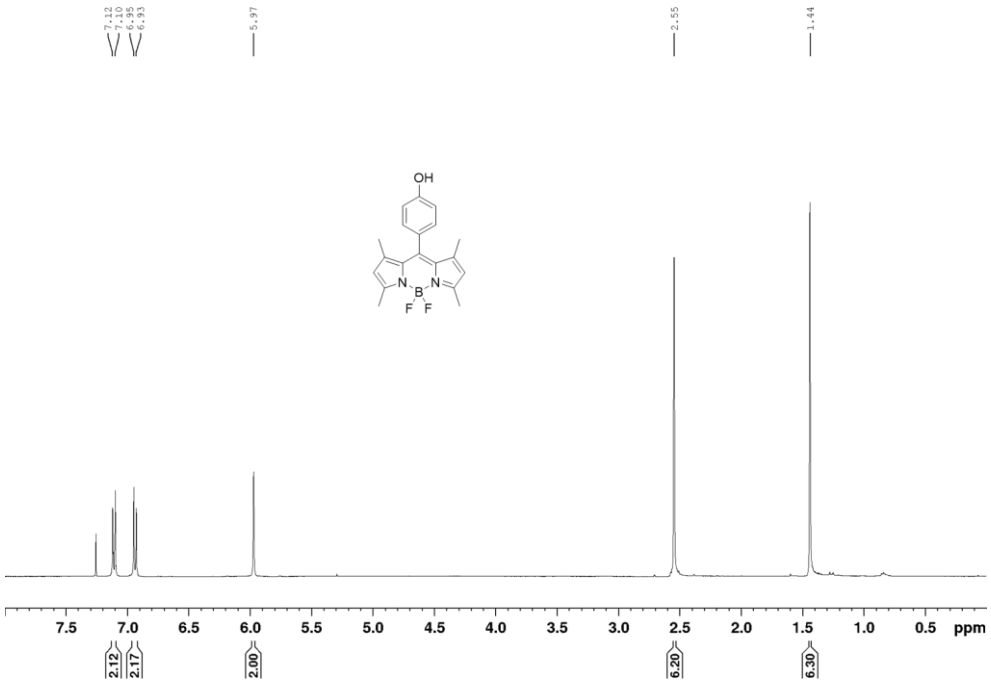

Figure S1. ^{1}H-NMR spectrum (400 MHz, 298K) of **1** in $CDCl_3$.

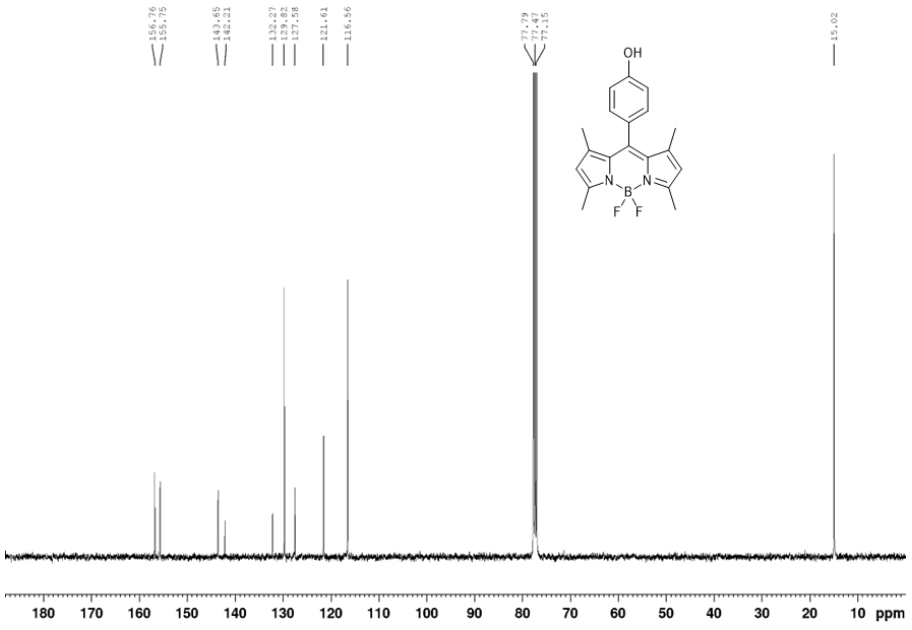

Figure S2. ^{13}C-NMR spectrum (100 MHz, 298K) of **1** in $CDCl_3$.

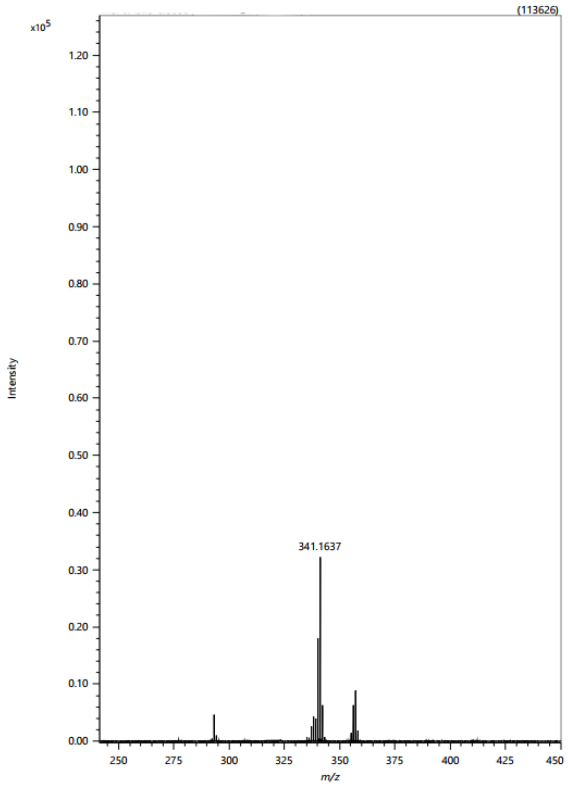

Figure S3. DART-HRMS spectrum of **1** in CH_2Cl_2.

*1.1.2 Synthesis of 8-[4-(10-bromodecyloxy) phenyl]-1,3,5,7-tetramethyl-4,4-difluoro-4-bora-3a,4a-diaza-s-indacene (**2**)*

Compound **1** (0.500 g, 1.50 mmol) and 1,10-dibromodecane (0.4 mL, 2.20 mmol) were dissolved in acetone (15 mL) with potassium carbonate (0.203 g, 1.50 mmol). The resulting mixture was refluxed for 18 h. The reaction was quenched by the addition of water, and the product was extracted with CH_2Cl_2. The combined organic extracts were dried over anhydrous Na_2SO_4, and the solvent was evaporated. The crude product was purified by silica gel column chromatography with 3:2 CH_2Cl_2/hexane as the eluent to afford compound **2** as an orange solid (0.532 g, 0.95 mmol, 63%). **^{1}H-NMR** (400 MHz, $CDCl_3$, ppm): δ = 7.14 (d, J = 8.6 Hz, 2H; $CH_{aromatic}$), 6.98 (d, J = 8.6 Hz, 2H; $CH_{aromatic}$), 5.97 (s, 2H; CH), 3.99 (t, J = 6.5 Hz, 2H; CH_2), 3.41 (t, J = 6.8 Hz, 2H; CH_2), 2.54 (s, 6H; CH_3), 1.87–1.80 (m, 4H; CH_2), 1.52–1.29 (m, 18H; CH_2 and CH_3). **^{13}C-NMR** (100 MHz, $CDCl_3$, ppm): δ=160.2, 156.6, 145.5, 141.8, 131.8, 129.1, 126.5, 115.5, 85.6, 68.3, 34.2, 32.9, 29.5, 29.4, 29.3, 28.9, 28.2, 26.13, 17.3, 16.1. **DART-HRMS** (ESI) *m/z*: calcd. for $C_{27}H_{35}BBrF_2N_2O^+$ $[M+H]^+$, 559.2301; found. 559.2279.

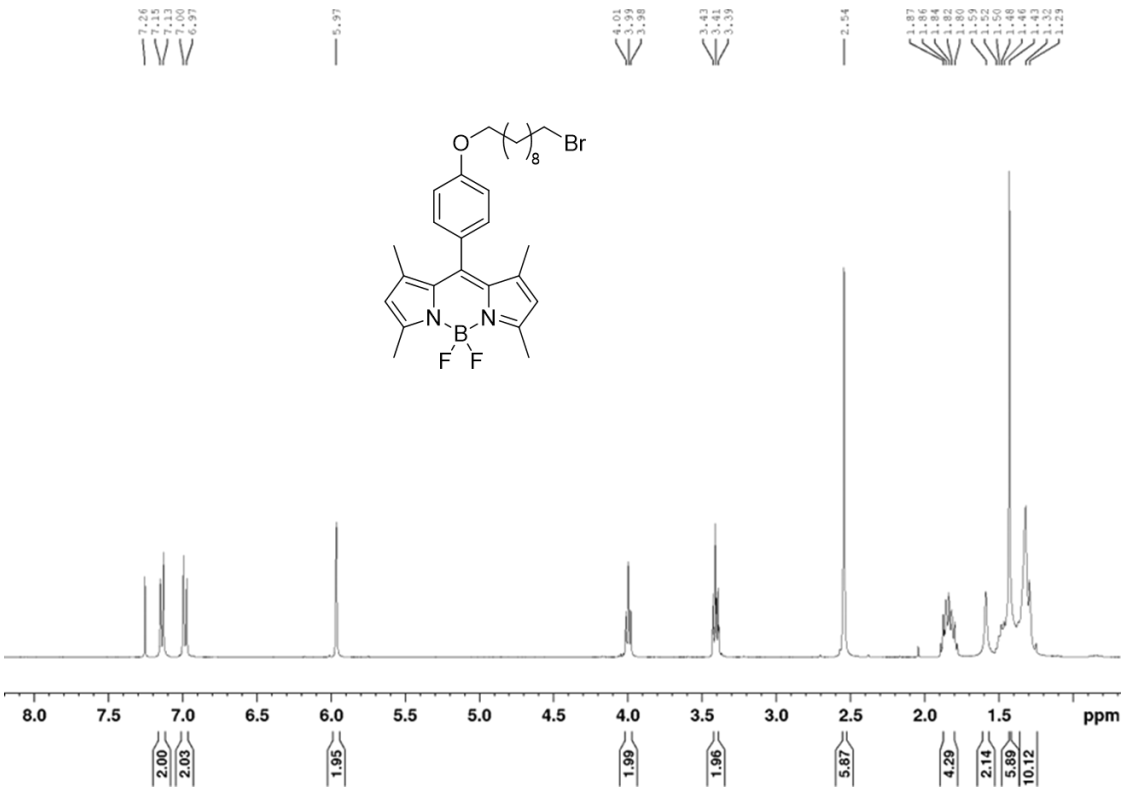

Figure S4. ^{1}H-NMR spectrum (400 MHz, 298K) of **2** in $CDCl_3$.

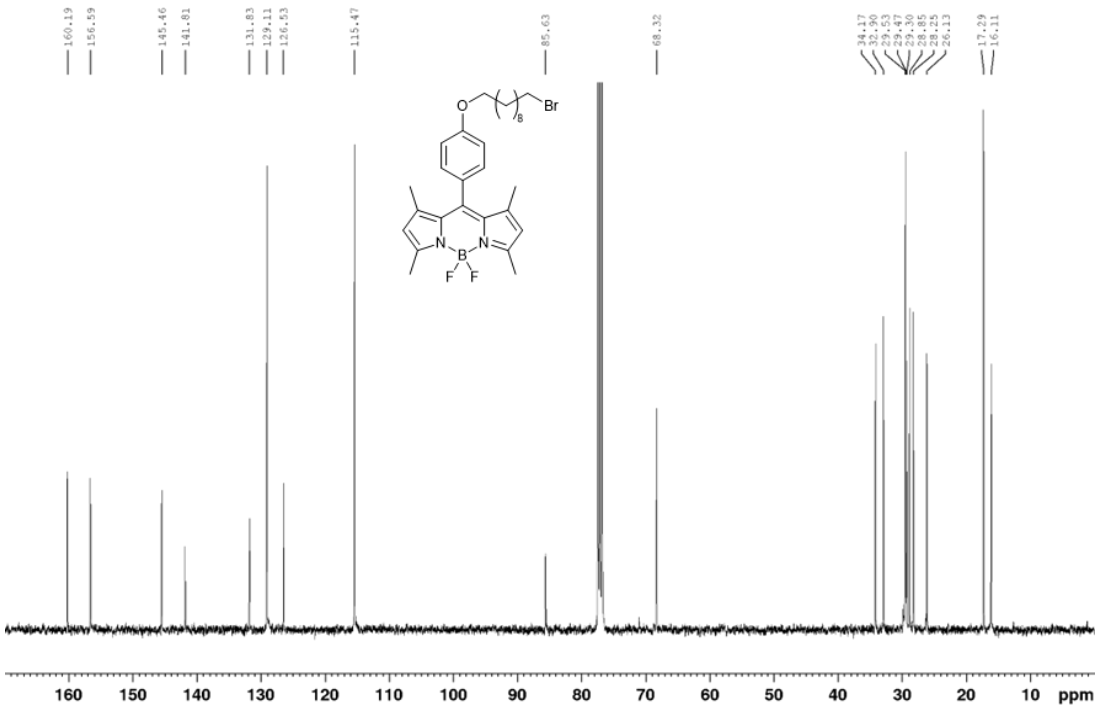

Figure S5. ^{13}C-NMR spectrum (100 MHz, 298K) of **2** in $CDCl_3$.

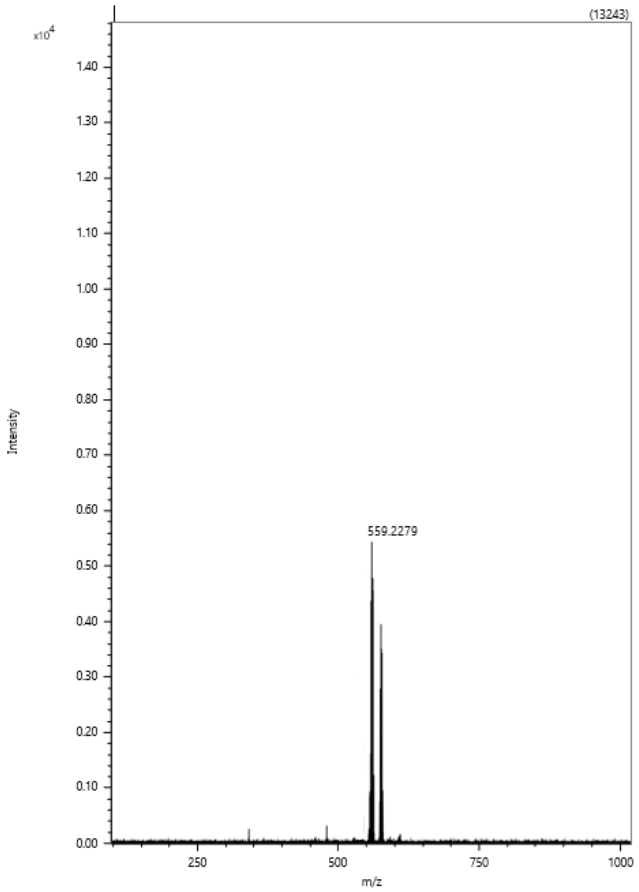

Figure S6. DART-HRMS spectrum of **2** in CH_2Cl_2.

*1.1.3 Synthesis of 8-[4-(10-bromodecyloxy)phenyl]-2,6-diiodo-1,3,5,7-tetramethyl-4,4-difluoro-4-bora-3a,4a-diaza-s-indacene (**3**)*

Compound **2** (0.350 g, 0.62 mmol) and *N*-iodosuccinimide (0.444 g, 1.98 mmol) were dissolved in CH_2Cl_2 (30 mL). The reaction mixture was stirred at room temperature for 18 h. The crude product was extracted with CH_2Cl_2 and water (3 × 30 mL). The combined organic layer was dried over anhydrous Na_2SO_4, concentrated under reduced pressure, and purified by silica gel column chromatography, eluting with 1:3 CH_2Cl_2/hexane, to afford compound **3** as a red solid (0.517 g, 0.63 mmol, 97%). **^{1}H–NMR** (400 MHz, $CDCl_3$, ppm): δ =7.11 (d, J = 8.6 Hz, 2H; $CH_{aromatic}$), 7.01 (d, J = 8.6 Hz, 2H; $CH_{aromatic}$), 4.01 (t, J = 6.5 Hz, 2H; CH_2), 3.41 (t, J = 6.8 Hz, 2H; CH_2), 2.63 (s, 6H; CH_3), 1.89–1.79 (m, 4H; CH_2), 1.49–1.25 (m, 18H; CH_2 and CH_3). **^{13}C-NMR** (100 MHz, $CDCl_3$, ppm): δ = 160.2, 156.6, 145.5, 141.8, 131.8, 129.1, 126.53, 115.5, 85.6, 68.3, 34.2, 32.9, 29.5, 29.3, 28.9, 28 .3, 26.1, 17.3, 16.1. **DART-HRMS** (ESI) *m/z*: calcd. for $C_{27}H_{33}BBrF_2I_2N_2O^+$ $[M]^+$, 810.0161; found, 810.0105.

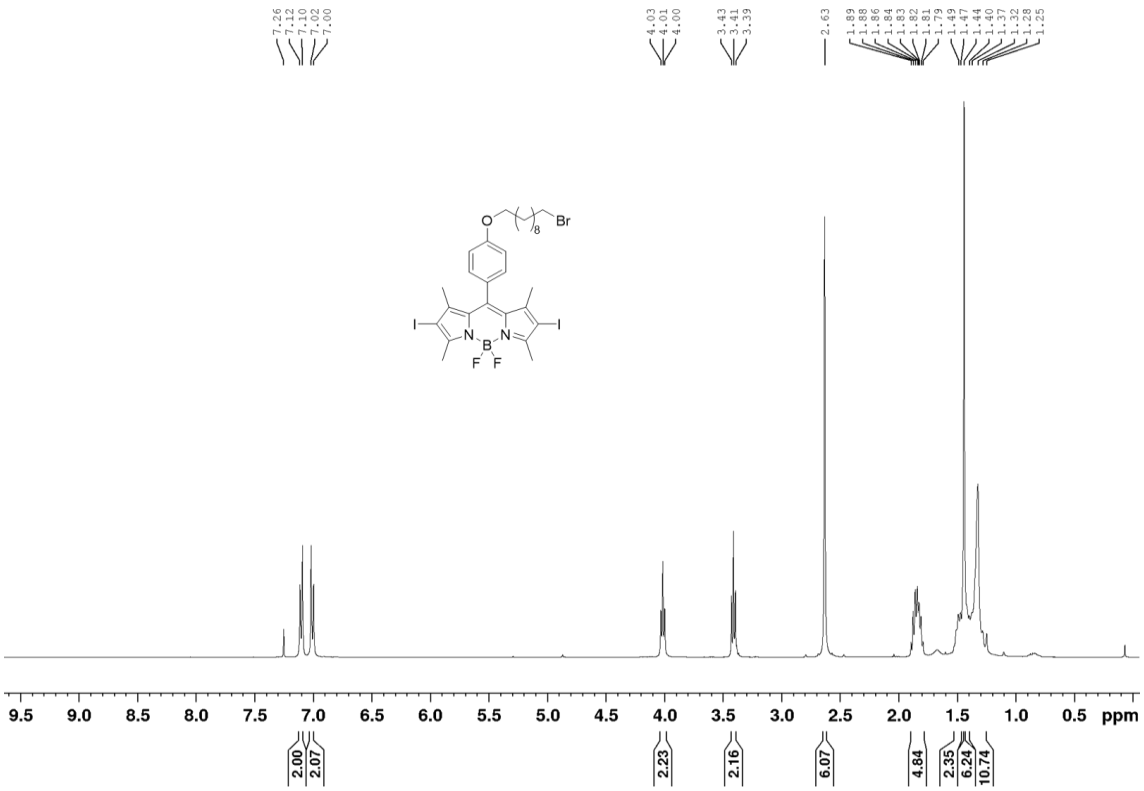

Figure S7. ^{1}H-NMR spectrum (400 MHz, 298K) of **3** in $CDCl_3$.

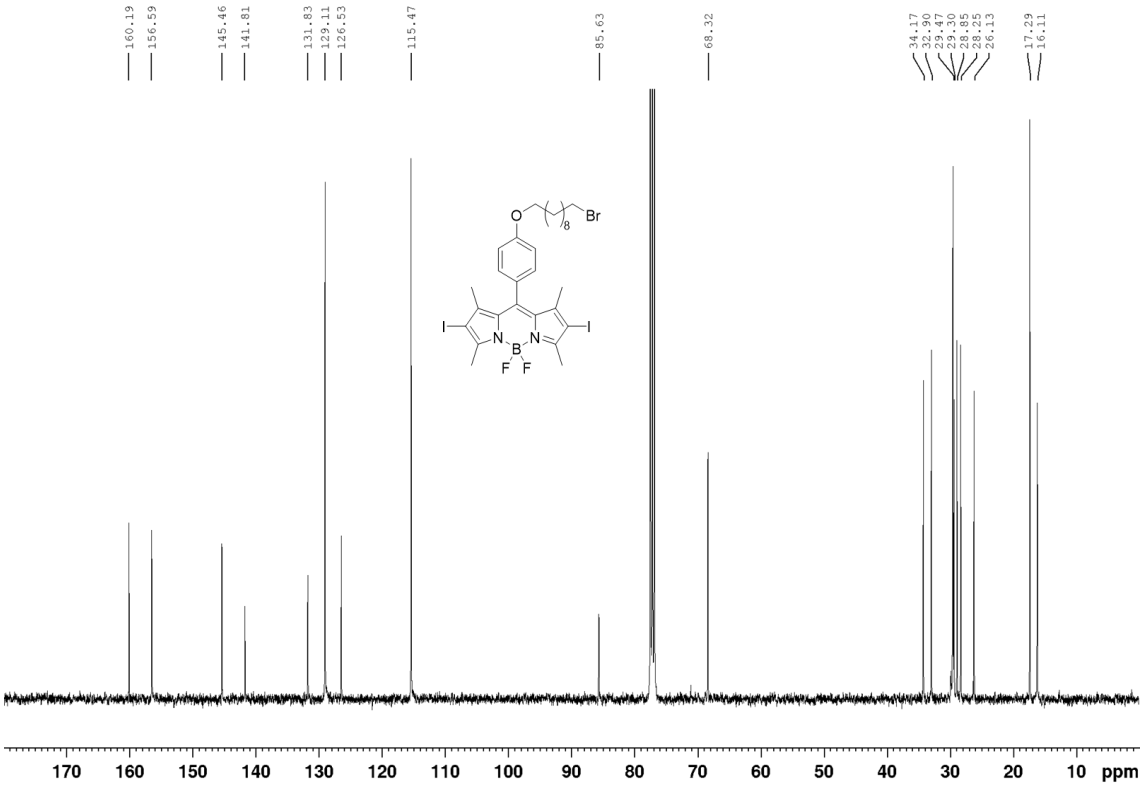

Figure S8. ^{13}C-NMR spectrum (100 MHz, 298K) of **3** in $CDCl_3$.

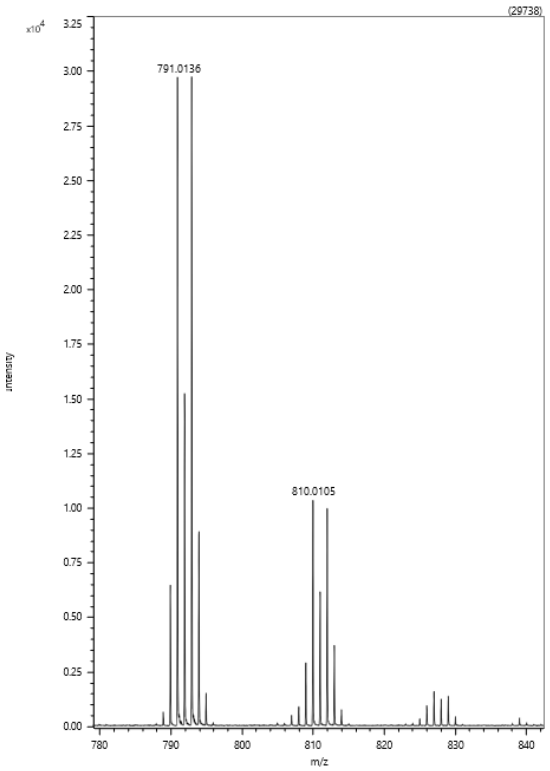

Figure S9. DART-HRMS spectrum of **3** in CH_2Cl_2.

*1.1.4 Synthesis of 8-[4-(10-bromodecyloxy)phenyl]-2,6-diiodo-3,5-bis(4-methoxyphenyl)-1,7-dimethyl-4,4-difluoro-4-bora-3a,4a-diaza-s-indacene (**4**)*

Compound **3** (0.080 g, 0.10 mmol) and 4-methoxybenzaldehyde (0.060 g, 0.44 mmol) were dissolved in dry CH_3CN (10 mL). Glacial acetic acid (0.2 mL, 3.84 mmol) and piperidine (0.2 mL, 2.67 mmol) were added to the solution. The resulting mixture was refluxed for 4 h. After cooling, the solvent was evaporated under reduced pressure, and the residue was diluted with H_2O (20 mL) and extracted with CH_2Cl_2 (3 × 30 mL). The combined organic extracts were dried over anhydrous Na_2SO_4 and concentrated under reduced pressure. The crude product was purified by column chromatography on silica gel, eluting with 1:1 CH_2Cl_2/hexane, to yield compound **4** as a dark green solid (0.025 g, 0.02 mmol, 25%). **^{1}H-NMR** (400 MHz, $CDCl_3$, ppm): δ = 8.13 (d, J = 16.6 Hz, 2H; C=CH), 7.58 (d, J = 8.61 Hz, 4H; $CH_{aromatic}$), 7.55 (d, J = 16.12 Hz, 2H; C=CH), 7.15 (d, J = 8.54 Hz, 2H; $CH_{aromatic}$), 7.03 (d, J = 8.59 Hz, 2H; $CH_{aromatic}$), 6.95 (d, J = 8.61 Hz, 4H; $CH_{aromatic}$), 4.03 (t, J = 6.6 Hz, 2H; CH_2), 3.86 (s, 6H; CH_3), 3.42 (t, J = 6.8 Hz, 2H; CH_2), 1.88–1.82 (m, 4H; CH_2), 1.51–1.25 (m, 18H; CH_2 and CH_3). **^{13}C-NMR** (100 MHz, $CDCl_3$, ppm): δ = 160.8, 160.2, 150.4, 145.8, 138.9, 138.8, 135.6, 133.2, 129.7, 129.6, 129.3, 127.1, 116.8, 115.4, 114.3, 82.57, 68.3, 53.4, 32.9, 29.8, 29.4, 29.2, 28.8, 28.1, 26.1, 17.1. **HRMS** (ESI) *m/z*: calcd. for $C_{43}H_{44}BBrF_2I_2N_2O_3^+$ $[M]^+$, 1046.0999; found, 1046.1030.

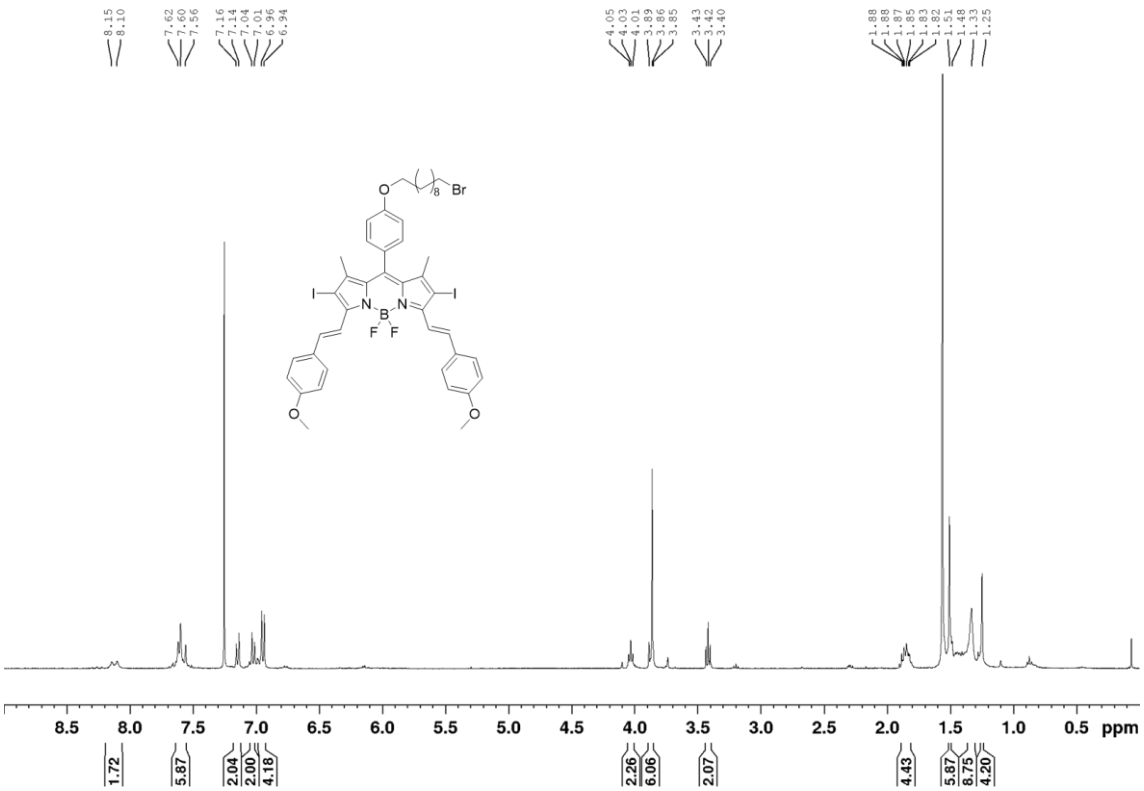

Figure S10. ^{1}H-NMR spectrum (400 MHz, 298K) of **4** in $CDCl_3$.

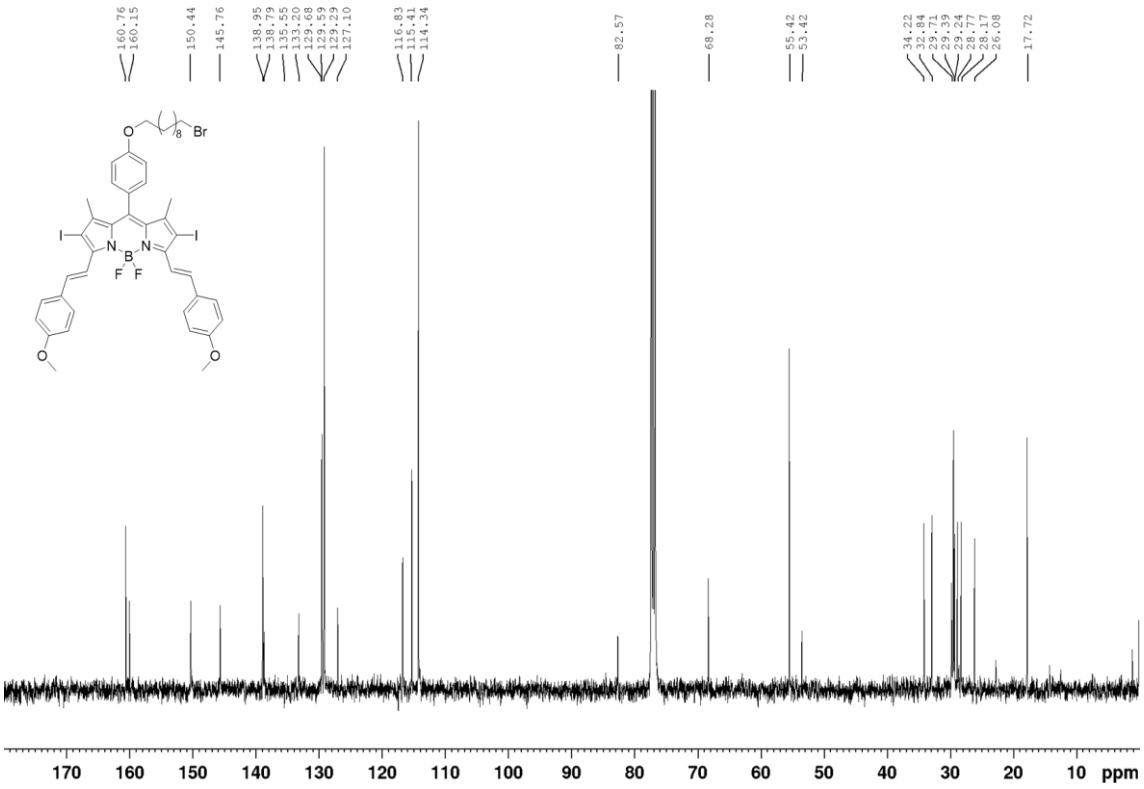

Figure S11. ^{13}C-NMR spectrum (100 MHz, 298K) of **4** in $CDCl_3$.

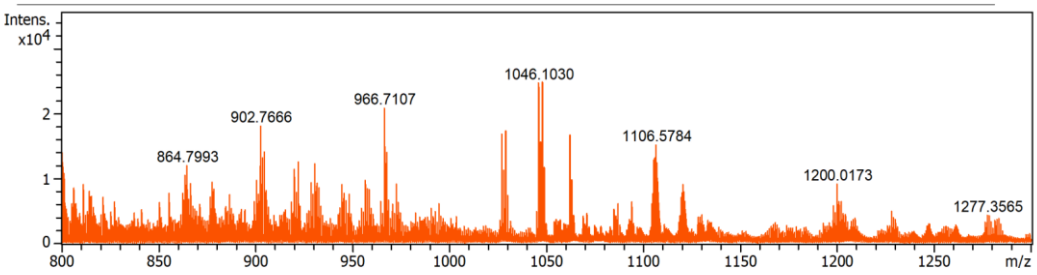

Figure S12. ESI-HRMS spectrum of **4** in CH_2Cl_2.

*1.1.5 Synthesis of 8-[4-(10-(trimethylammonio)decyloxy)phenyl]-2,6-diiodo-3,5-bis(4-methoxyphenyl)-1,7-dimethyl-4,4-difluoro-4-bora-3a,4a-diaza-s-indacene bromide (**PS3**)*

Compound **4** (0.015 g, 0.015 mmol) and 3 M trimethylamine in isopropanol (0.1 ml, 0.03 mmole) were dissolved in 10 mL 1:1 $CHCl_3$/ethanol. The resulting mixture was heated at 80 °C for 18 h. After cooling, the mixture was concentrated under reduced pressure and purified by column chromatography (neutral alumina, 10:1 CH_2Cl_2/methanol) to give **PS3** as a dark green solid (0.016 g, 0.014 mmol, 93%). **^{1}H-NMR** (400 MHz, DMSO-d_6, ppm): δ = 8.06 (d, *J* = 16.6 Hz, 2H; C=CH), 7.58 (d, *J* = 8.8 Hz , 4H; $CH_{aromatic}$), 7.42 (d, *J* = 16.6 Hz, 2H; C=CH), 7.32 (d, *J* = 8.6 Hz, 2H; $CH_{aromatic}$), 7.12 (d, *J* = 8.6 Hz, 2H; $CH_{aromatic}$), 7.06 (d, *J* = 8.8 Hz, 4H; $CH_{aromatic}$), 4.05 (t, *J* = 6.3 Hz, 2H; CH_2), 3.82 (s, 6H; CH_3), 3.03 (s, 9H; CH_3), 1.70–1.62 (m, 4H; CH_2), 1.46 (s, 6H; CH_3), 1.34–1.22 (m, 12H; CH_2). **^{13}C-NMR** (100 MHz, DMSO-d_6, ppm): δ=161.2, 160.1, 150.2, 146.0, 139.1, 133.3, 130.1, 129.4, 126.5, 116.5, 115.9, 114.9, 84.7, 68.2, 65.8, 55.9, 55.4, 29.4, 29.2, 28.9, 26.2, 26.0, 22.5, 17.7. **HRMS** (ESI**,** *m/z)*: calcd. for $C_{46}H_{53}BF_2I_2N_3O_3$ $[M–Br]^+$ 1026.2545; found, 1026.2584.

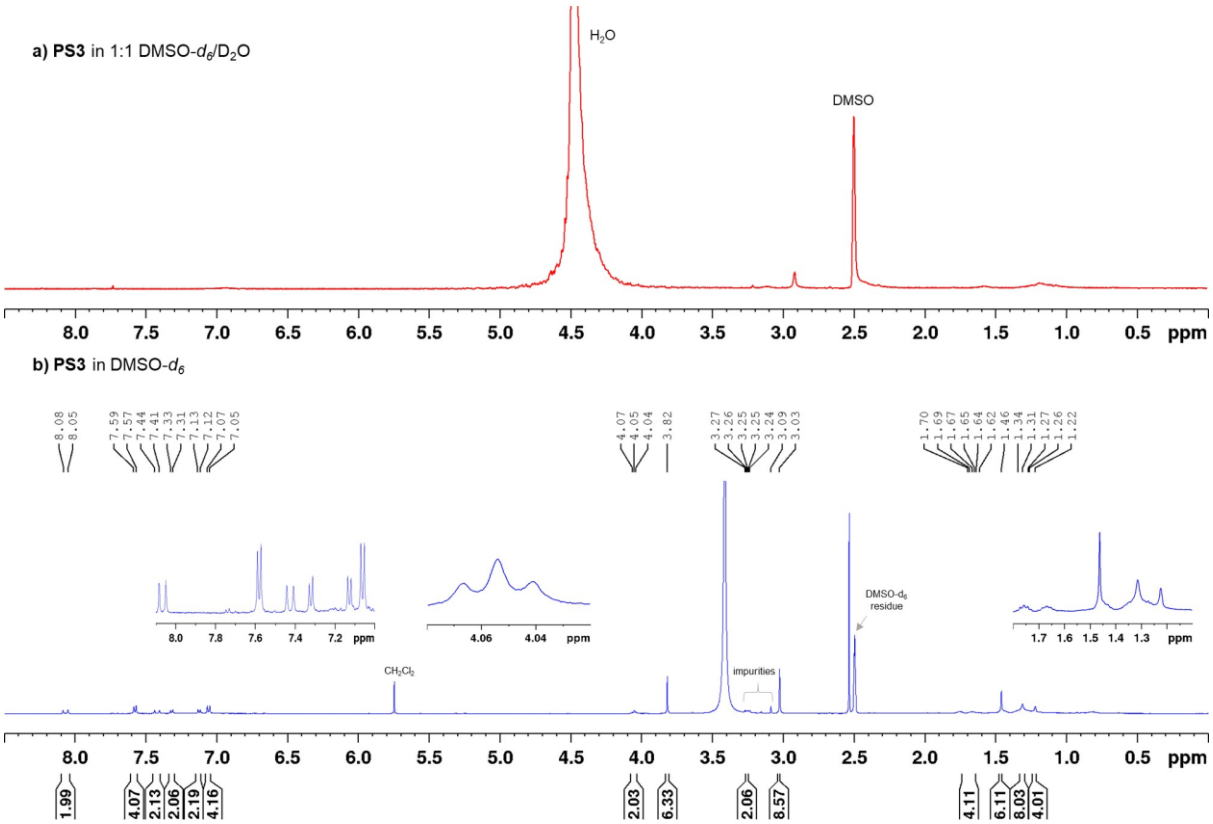

Figure S13. ^{1}H-NMR spectra (400 MHz, 298K) of **PS3** in (a) 1:1 DMSO-d_6/D_2O and (b) DMSO-d_6.

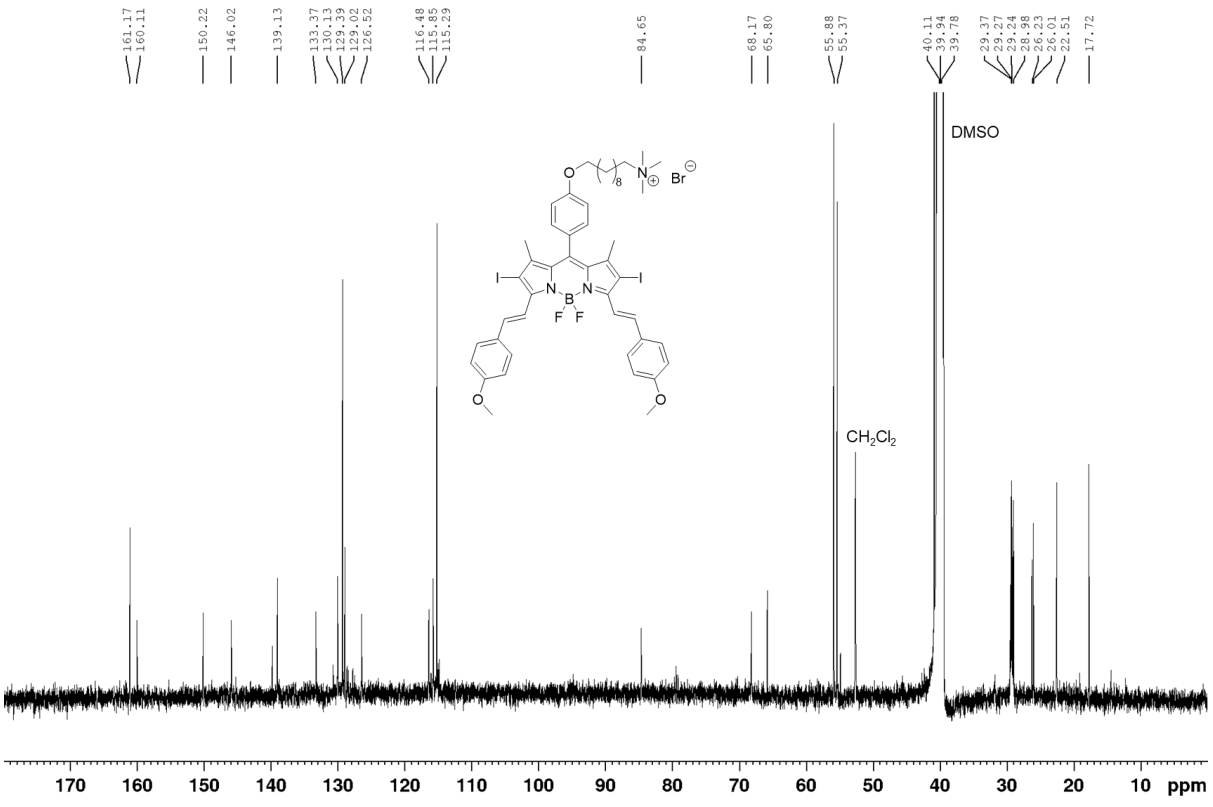

Figure S14. ^{13}C-NMR spectrum (100 MHz, 298K) of **PS3** in DMSO-d_6.

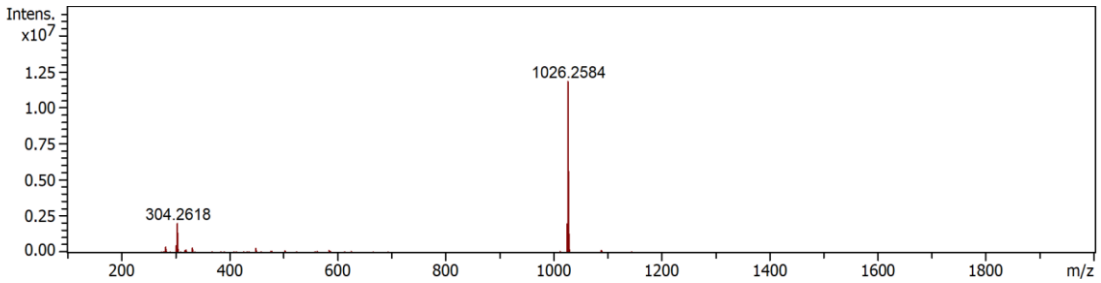

Figure S15. ESI-HRMS spectrum of **PS3** in CH_2Cl_2.

1.2 Synthesis of 2-azidoethyl 2,3,4,6-tetra-*O*-acetyl-*α*-D-mannopyranoside (7)

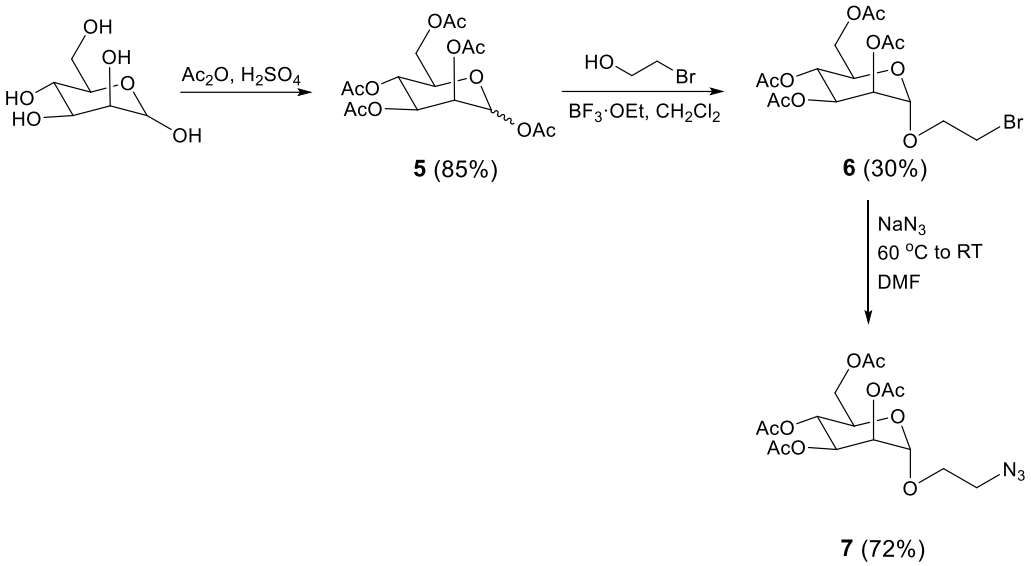

Scheme S2. Synthesis of **7**.

*1.2.1 Synthesis of 1,2,3,4,6-penta-O-acetyl-α-D-mannopyranoside (**5**)*

According to the literature,[3] D-mannose (2.00 g, 11 mmol) was suspended in acetic anhydride (12 mL, 110 mmol) at 0 ºC for 1 h. Two drops of 96% sulfuric acid were added, and the mixture was stirred at room temperature overnight. Water was then added to the mixture, and the product was extracted with dichloromethane. The organic extracts were washed with aqueous $NaHCO_3$ and water until the aqueous phase reached neutrality. The solvent was removed under reduced pressure to yield **5** as a pale-yellow oil (3.65 g, 9.3 mmol, 79%). **^{1}H-NMR** (400 MHz, $CDCl_3$, ppm): δ = 6.09 (d, J = 1.9 Hz, 1H; CH), 5.36–5.34 (m, 2H; CH), 5.26 (t, J = 2.0 Hz, 1H; CH), 4.31–4.26 (dd, 1H; CH), 4.01–4.13 (m, 2H; CH_2), 2.18 (s, 3H; CH_3), 2.17 (s, 3H; CH_3), 2.10 (s, 3H; CH_3), 2.05 (s, 3H; CH_3), 2.01 (s, 3H; CH_3). **^{13}C-NMR** (100 MHz, $CDCl_3$, ppm): δ 170.8 (C=O), 170.1 (C=O), 169.8 (C=O), 169.7 (C=O), 168.2 (C=O), 90.7 (O–C–O), 70.7 (C–O), 68.8 (C–O), 68.4 (C–O), 65.6 (C–O), 62.2 (C–O), 20.9 (CH_3),

20.8 (CH_3), 20.8 (CH_3), 20.7 (CH_3), 20.7 (CH_3). **LC-MS** (ESI) *m/z*: calcd. for $C_{16}H_{22}O_{11}Na^+$ $[M+Na]^+$, 413.1054; found, 413.1061.

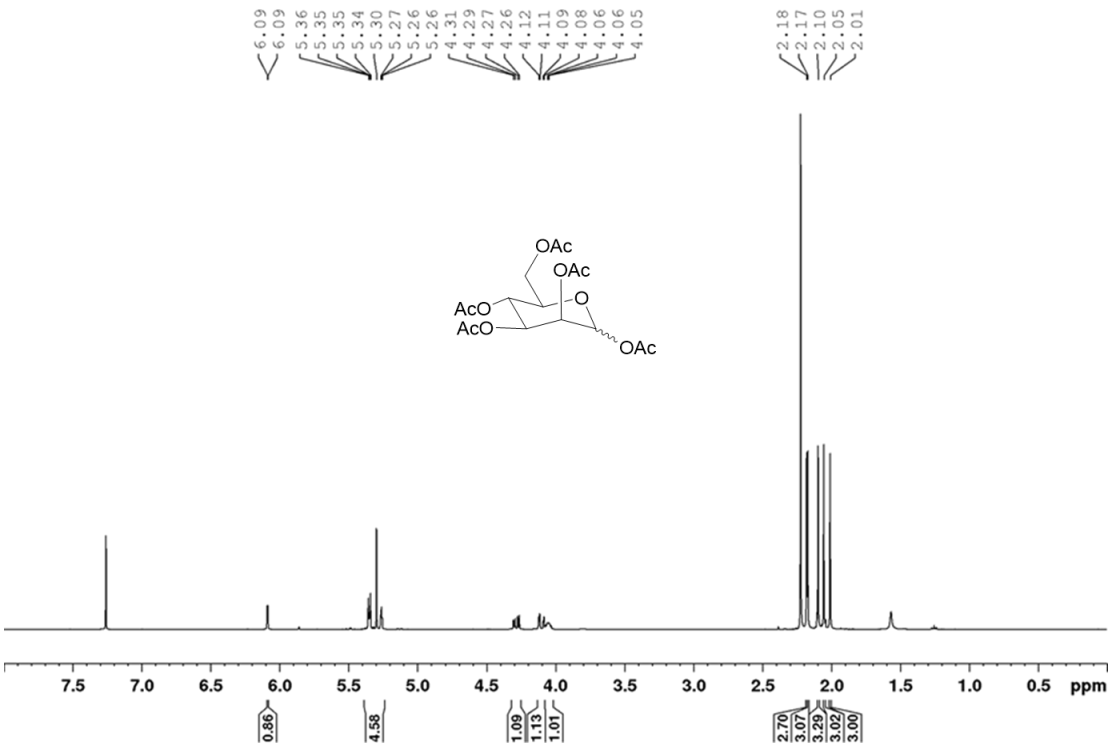

Figure S16. ^{1}H-NMR spectrum (400 MHz, 298K) of **5** in $CDCl_3$.

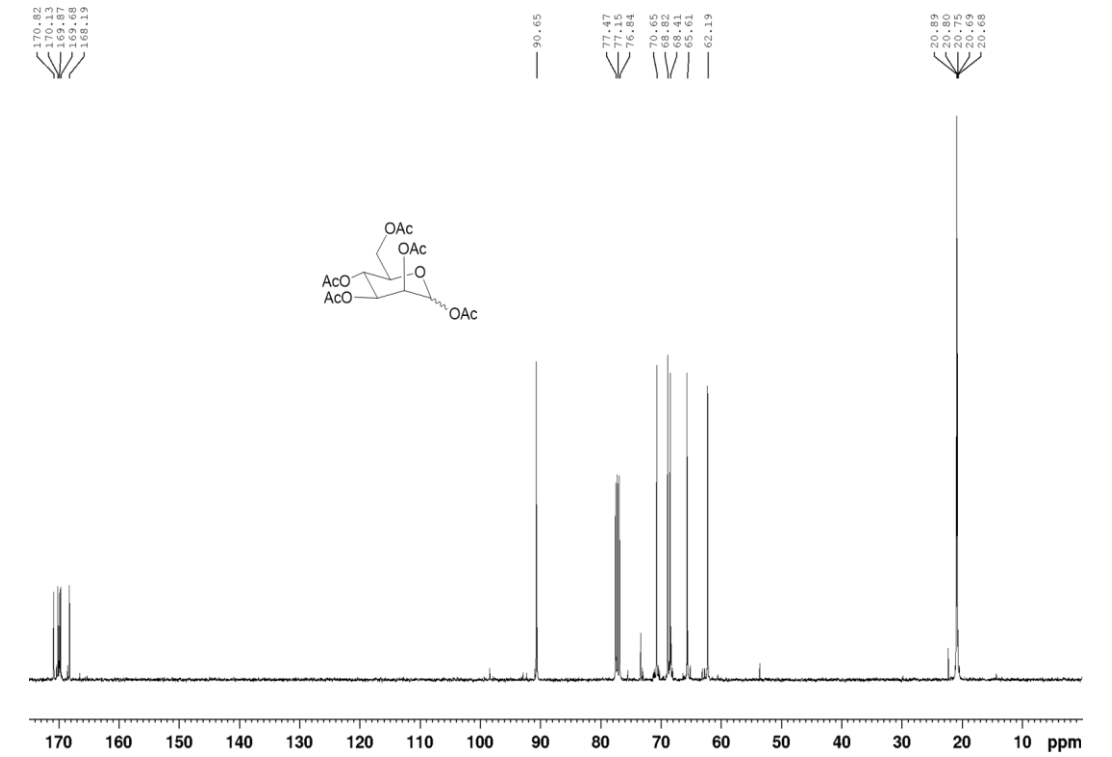

Figure S17.^{13}C-NMR spectrum (100 MHz, 298K) of **5** in $CDCl_3$.

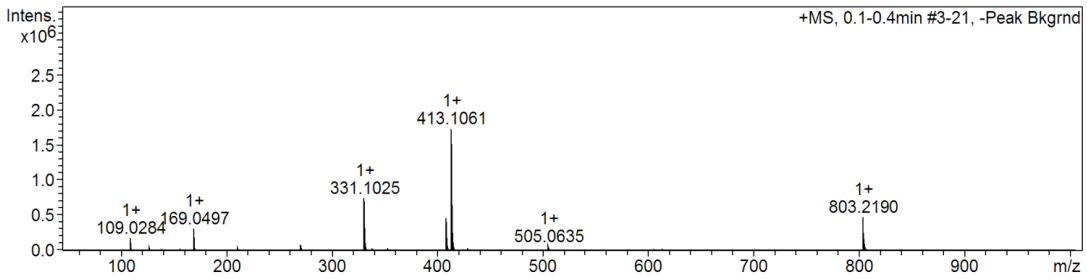

Figure S18. LC-MS spectrum of **5** in CH_2Cl_2.

*1.2.2 Synthesis of 2-bromoethyl 2,3,4,6-tetra-O-acetyl-α-D-mannopyranoside (**6**)*

Compound **5** (4.00 g, 10.2 mmol) and 2-bromoethanol (1.44 mL, 0.0204 mol) were mixed in dry CH_2Cl_2 (60 mL) under N_2 atmosphere at 0 °C. $BF_3{\cdot}OEt_2$ (6.28 mL, 51 mmol) was added, and the reaction mixture was stirred at 0 °C for 1 h and then at room temperature overnight. The reaction mixture was slowly added to cold water, and the organic layer was separated. The aqueous phase was extracted with CH_2Cl_2, and the combined organic layers were washed three times with aqueous $NaHCO_3$ and three times with water. The organic solution was dried over Na_2SO_4, and the solvent was removed under reduced pressure, yielding a yellow oil. Product **6** was then precipitated from cold diethyl ether as a white powder solid (1.40 g, 3.06 mmol, 20%). **^{1}H-NMR** (400 MHz, $CDCl_3$, ppm): δ = 5.34–5.27 (m, 3H; CH), 4.87 (d, J = 1.5 Hz, 1H; CH), 4.29–4.25 (dd, J = 5.4 Hz, 6.8 Hz, 2H; CH_2), 4.13 (dd, J = 1.8 Hz, 8.4 Hz, 2H; CH), 3.98 (dt, 1H; CH_2), 3.88 (dt, 1H; CH_2), 3.52 (t, J = 6.0 Hz, 2H; CH_2), 2.16 (s, 3H; CH_3), 2.11 (s, 3H; CH_3), 2.05 (s, 3H; CH_3), 2.00 (s, 3H; CH_3). **^{13}C-NMR** (100 MHz, $CDCl_3$, ppm): δ=170.7 (C=O), 170.1 (C=O), 169.9 (C=O), 169.8 (C=O), 97.8 (O–C–O), 69.4 (C–O), 69.0 (C–O), 68.9 (C–O), 68.5 (C–O), 66.0 (C–O), 62.4 (C–O), 29.7 (C–Br), 20.9 (CH_3), 20.8 (CH_3), 20.7 (CH_3), 20.7 (CH_3). **LC-MS** (ESI) *m/z*: calcd. for $C_{16}H_{22}O_{11}Na^+$ $[M+Na]^+$, 477.0367, found 477.0369.

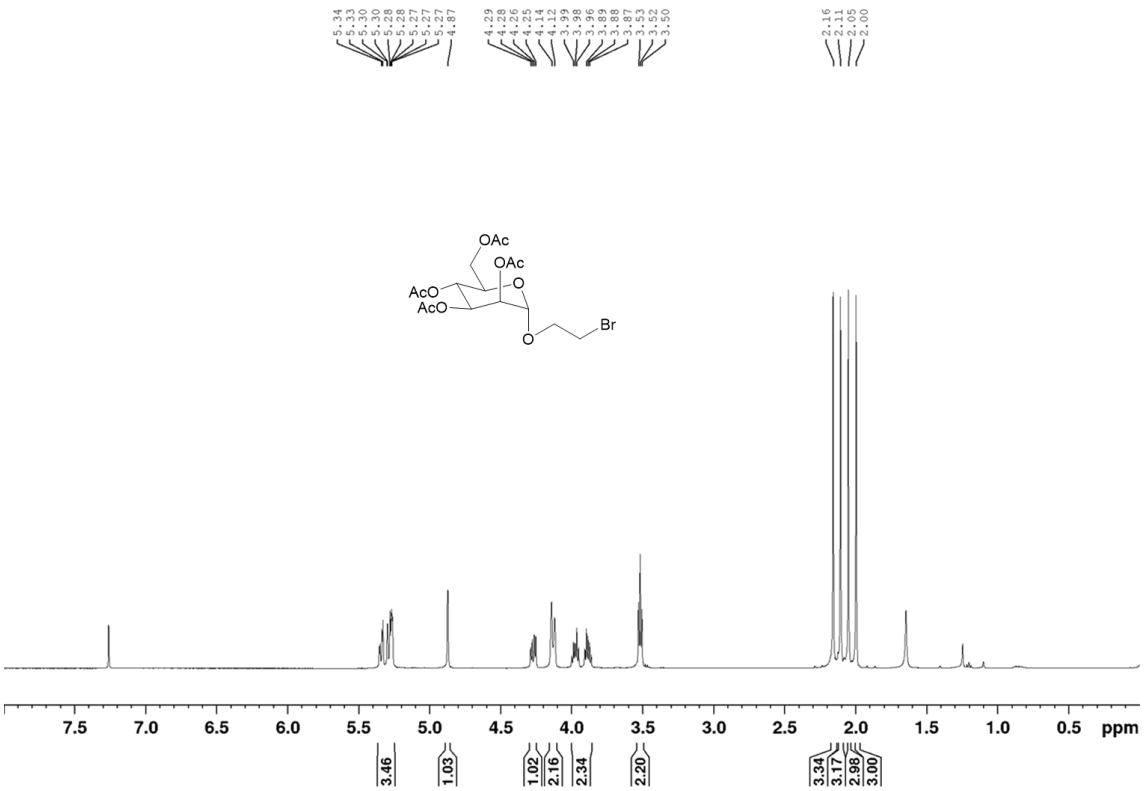

Figure S19. ^{1}H-NMR spectrum (400 MHz, 298K) of **6** in $CDCl_3$.

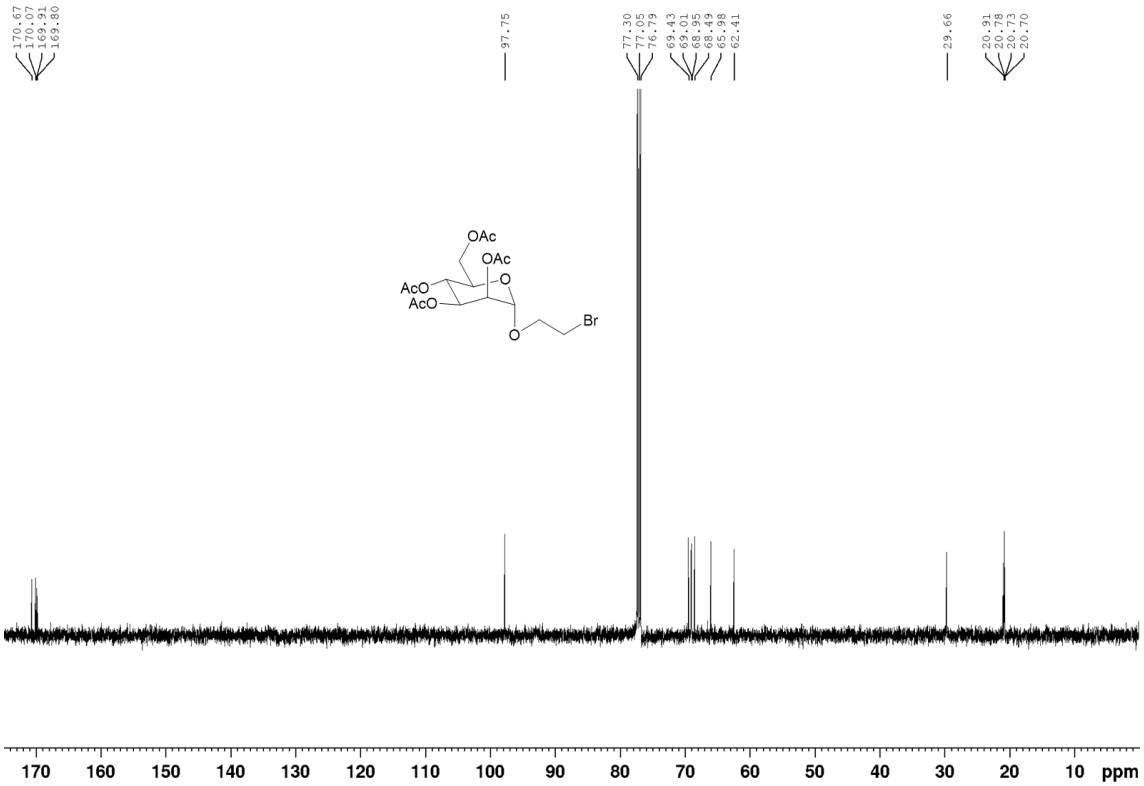

Figure S20. ^{13}C-NMR spectrum (100 MHz, 298K) of **6** in $CDCl_3$.

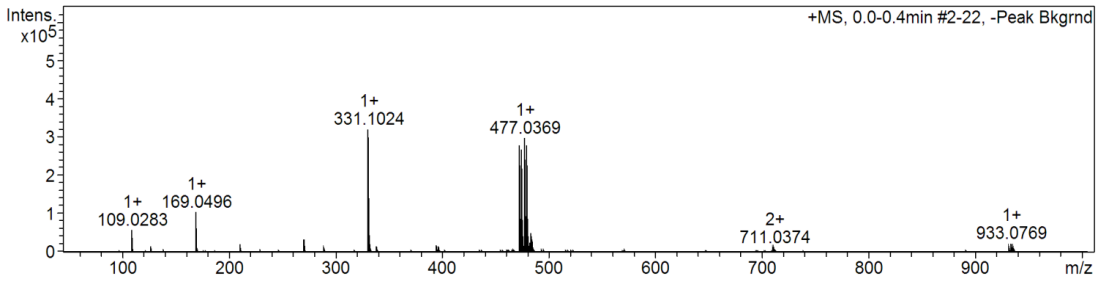

Figure S21. LC-MS spectrum of **6** in CH_2Cl_2.

*1.2.3 Synthesis of 2-azidoethyl 2,3,4,6-tetra-O-acetyl-α-D-mannopyranoside (**7**)*

Compound **6** (2.00 g, 4.4 mmol) and sodium azide (2.28 g, 35.12 mmol) were stirred in dry DMF (30 mL) under a nitrogen atmosphere at 60 °C for 6 h and then at room temperature overnight. The crude product was extracted with ethyl acetate and washed three times with water and three times with brine. The combined organic phase was dried over Na_2SO_4, and the solvent was removed under reduced pressure. Compound **7** was obtained as a white solid without further purification (1.59 g, 3.80 mmol, 80%). **^{1}H-NMR** (400 MHz, $CDCl_3$, ppm): δ = 5.38–5.27 (m, 3H; CH), 4.87 (d, *J* = 1.5 Hz, 1H; CH), 4.31–4.27 (dd, *J* = 5.4 Hz, 7.0 Hz, 1H; CH_2), 4.14–4.10 (dd, *J* = 2.4 Hz, 9.8 Hz, 1H; CH_2), 4.06–4.02 (m, 1H; CH), 3.89–3.84 (ddd, 1H; CH), 3.69–3.64 (ddd, 1H; CH_2), 3.49–3.44 (m, 2H; CH_2), 2.16 (s, 3H; CH_3), 2.11 (s, 3H; CH_3), 2.05 (s, 3H; CH_3), 2.00 (s, 3H; CH_3). **^{13}C-NMR** (100 MHz, $CDCl_3$, ppm): δ = 170.8 (C=O), 170.1 (C=O), 169.9 (C=O), 169.9 (C=O), 97.8 (O–C–O), 69.5 (C–O), 68.9 (C–O), 67.2 (C–O), 66.1 (C–O), 62.5 (C–O), 50.4 (C–N), 20.9 (CH_3), 20.9 (CH_3), 20.8 (CH_3), 20.8 (CH_3). **LC–MS** (ESI) *m/z*: calcd. for $C_{16}H_{22}O_{11}Na^+$ $[M+Na]^+$, 440.1276, found, 440.1280.

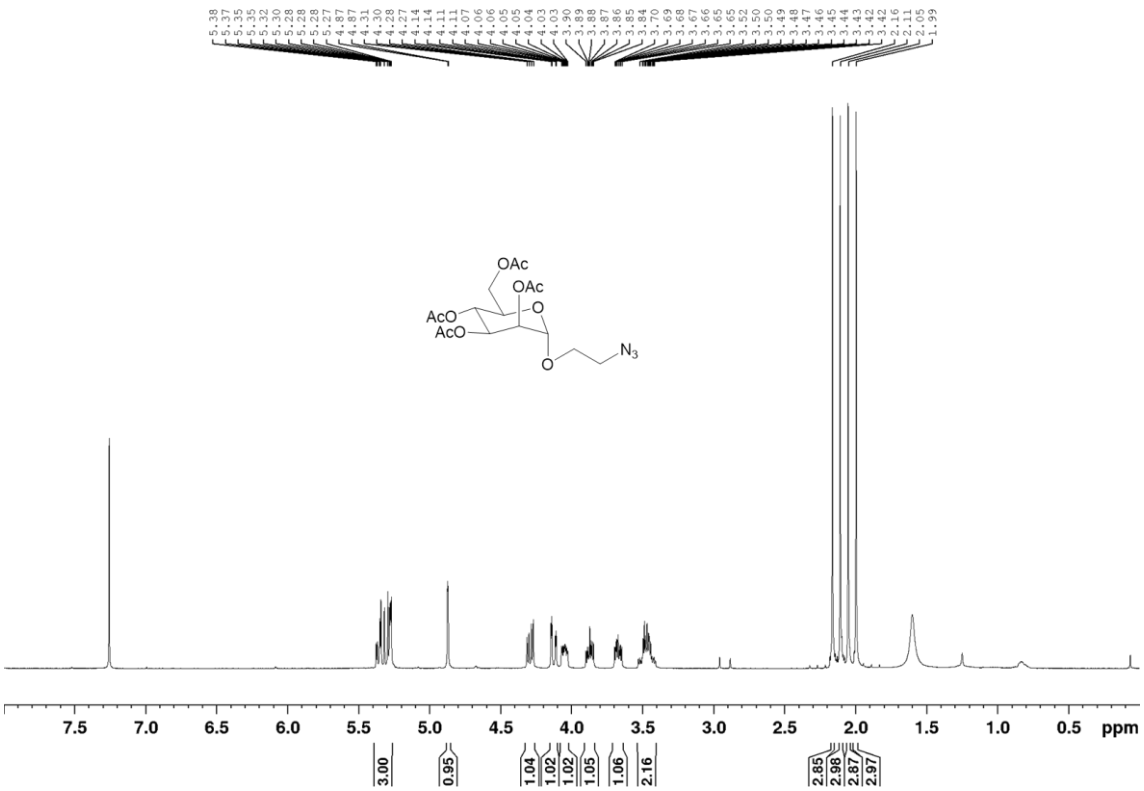

Figure S22. ^{1}H-NMR spectrum (400 MHz, 298K) of **7** in $CDCl_3$.

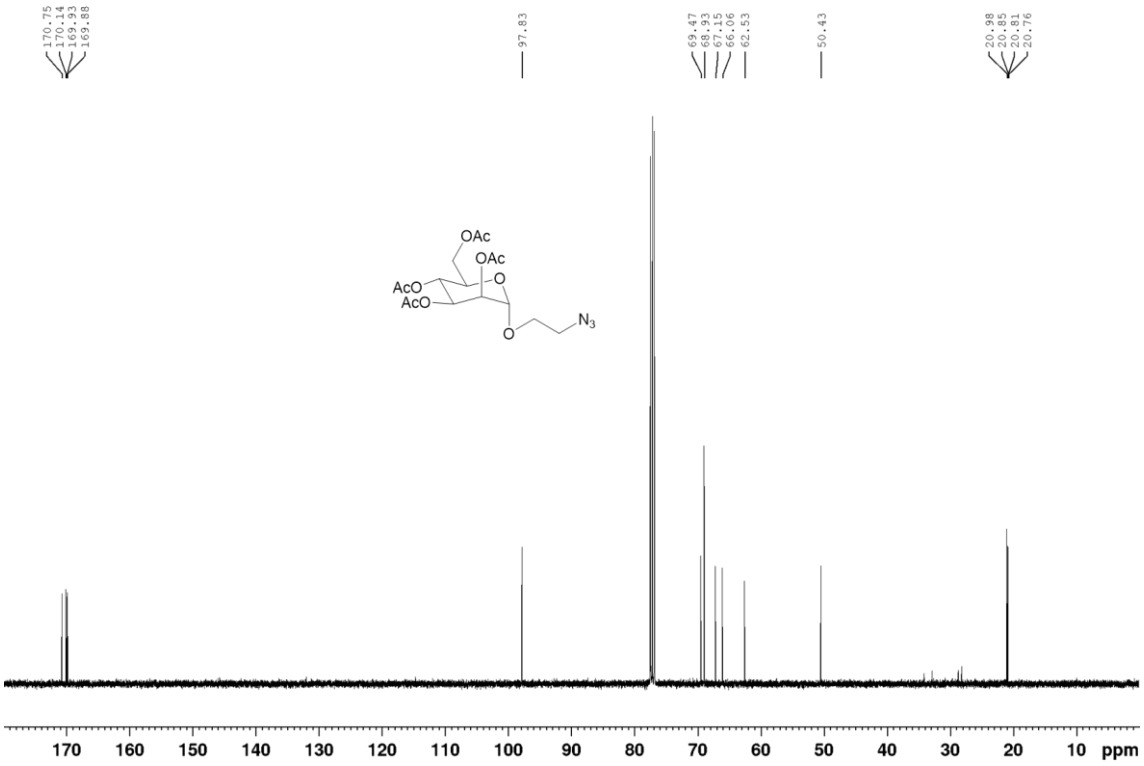

Figure S23. ^{13}C-NMR spectrum (100 MHz, 298K) of **7** in $CDCl_3$.

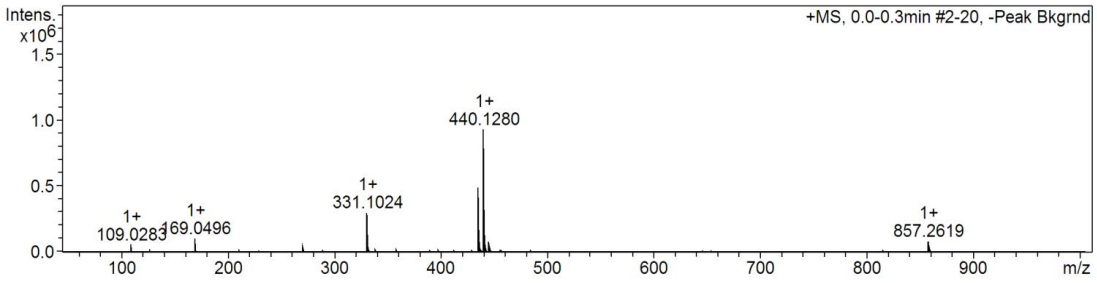

Figure S24. LC-MS spectrum of **7** in CH_2Cl_2.

1.3 Synthesis of WP5

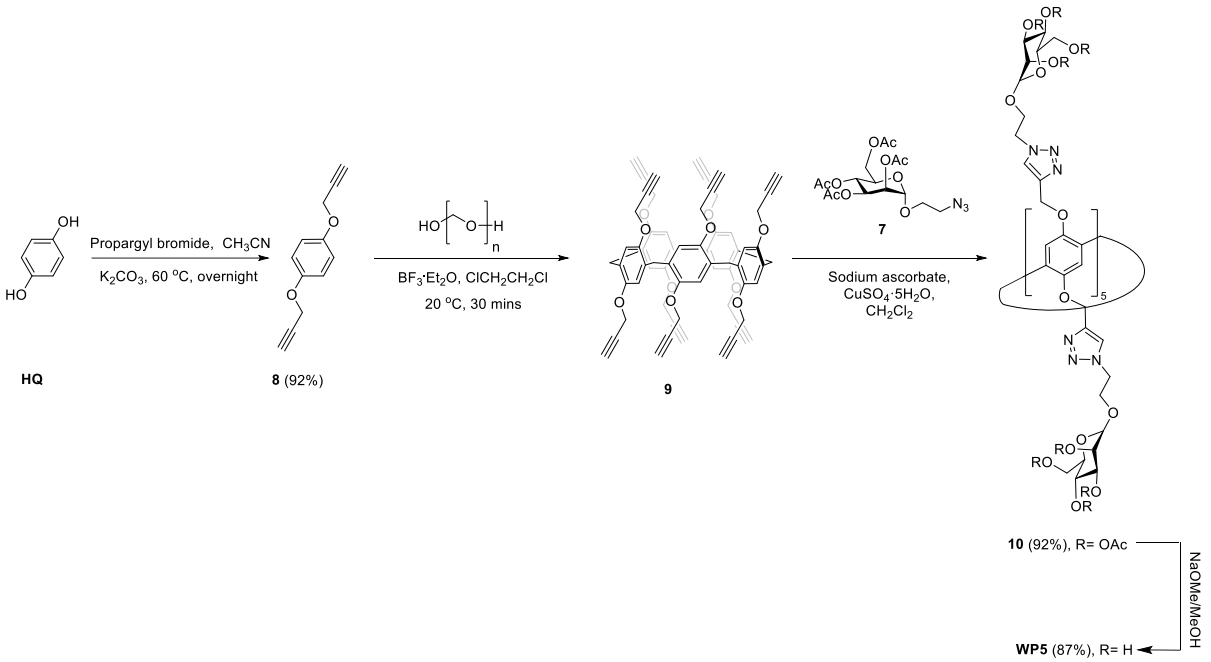

Scheme S3. Synthesis of **WP5**.

*1.3.1 Synthesis of 1,4-bis(prop-2-yn-1-yloxy)benzene (**8**)*

Compound **8** was prepared according to the literature.[4] Hydroquinone (**HQ**) (3.00 g, 0.03 mol) was dissolved in CH_3CN (100 mL) under a nitrogen atmosphere. K_2CO_3 (3.7 g**,** 0.027 mol) was added, and the reaction mixture was stirred at 60 °C for 2 h. Propargyl bromide (12.4 mL, 0.163 mol) was then added, and the reaction mixture was stirred at 60 °C for 24 h. Following solvent removal, the resulting solid was dissolved in a mixture of ethyl acetate and water. The organic layer was dried over anhydrous $MgSO_4$. After the solvent was removed, the crude product was purified by silica gel column chromatography, eluting with 1:1 CH_2Cl_2/hexane, to give **8** as a light-yellow solid (4.63 g, 0.03 mol, 92%). **^{1}H-NMR** (400 MHz, $CDCl_3$, ppm) δ = 6.94 (s, 4H; $CH_{aromatic}$), 4.66 (d, J = 2.4 Hz, 4H; CH_2), 2.52 (t, J = 2.4 Hz, 2H; CH).

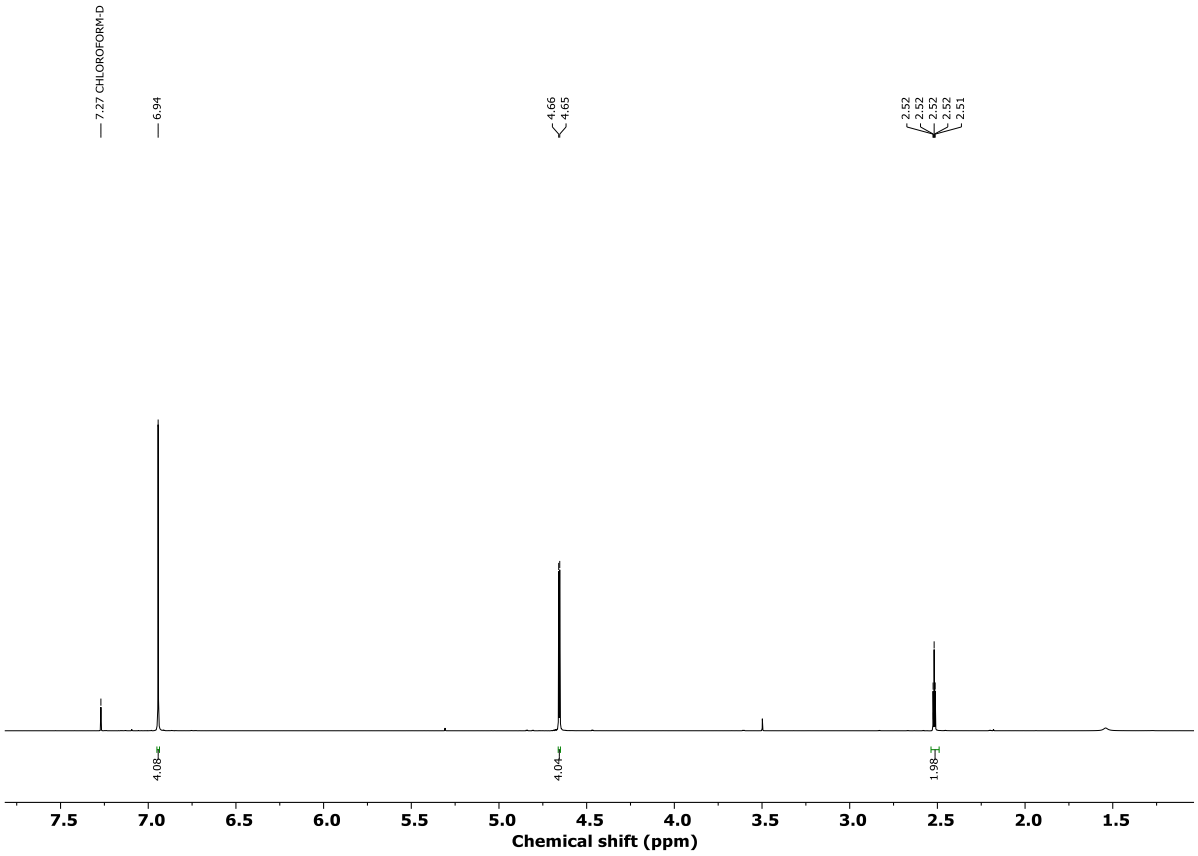

Figure S25. ^{1}H-NMR spectrum (400 MHz, 298K) of **8** in $CDCl_3$.

*1.3.2 Synthesis of alkyne-substituted pillar[5]arene (**9**)*

Compound **9** was prepared according to the literature.[4] Compound **8** (1.86 g, 10 mmol) was dissolved in 1,2-dichloroethane (20 ml), followed by addition of finely ground paraformaldehyde (0.90 g, 30 mmol). The suspension was stirred at room temperature. $BF_3{\cdot}Et_2O$ (1.41 ml, 10 mmol) was subsequently added slowly to produce a greenish solution. The reaction mixture was stirred for 30 mins, then poured into water. The organic residue was extracted into CH_2Cl_2 (3 x 30 ml), washed with water (3 x 50 ml), and dried over Na_2SO_4. After the solvent was removed, the crude product was purified on a silica gel column, eluting with 3:2 CH_2Cl_2/hexane, to afford **9** as a white powder (0.83 g, 4.20 mmol 42%). **^{1}H-NMR** (400 MHz, $CDCl_3$, ppm): δ = 6.83 (s, 10H; $CH_{aromatic}$), 4.54 (d, J = 2.4 Hz, 20H; CH_2), 3.82 (s, 10H; CH_2), 2.29 (t, J = 2.4 Hz, 10H; CH). **^{13}C-NMR** (100 MHz, $CDCl_3$, ppm): δ = 149.5, 115.6, 79.4, 75.0, 57.0, 29.8. **HRMS** (ESI) *m/z*: calcd. for $C_{65}H_{50}O_{10}$ $[M+H]^+$, 991.3477; found, 991.3464.

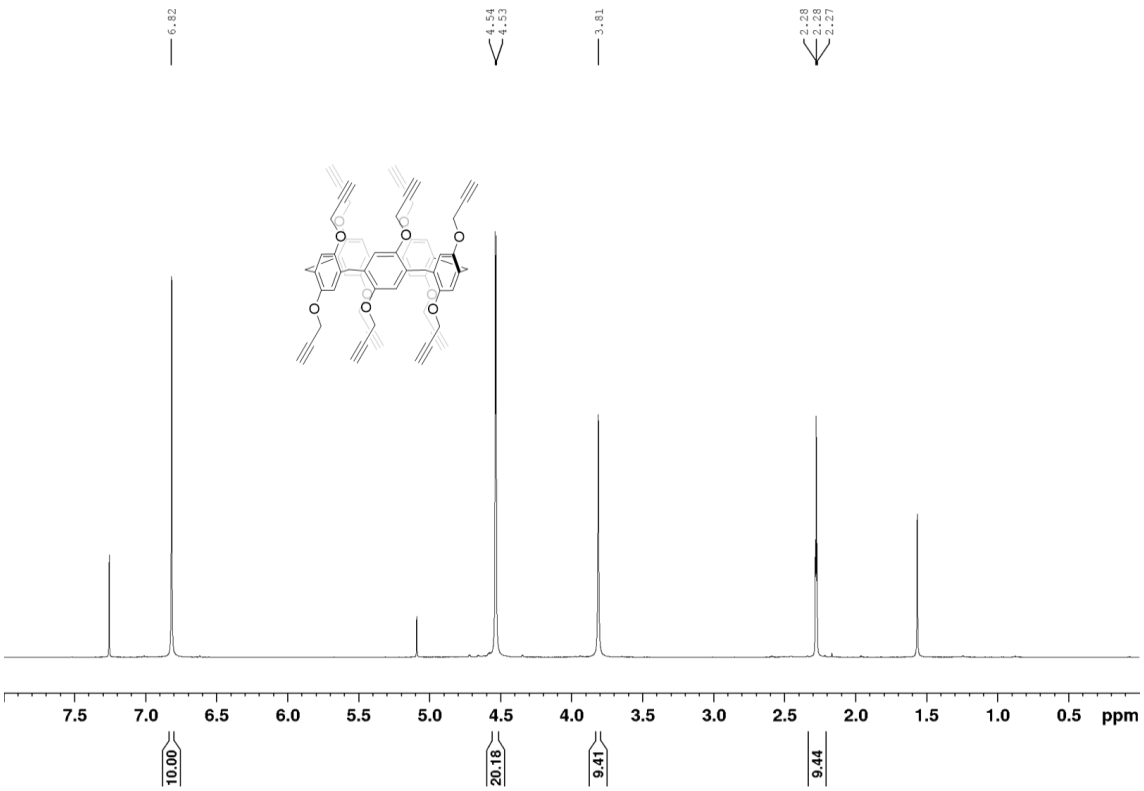

Figure S26. ^{1}H-NMR spectrum (400 MHz, 298K) of **9** in $CDCl_3$.

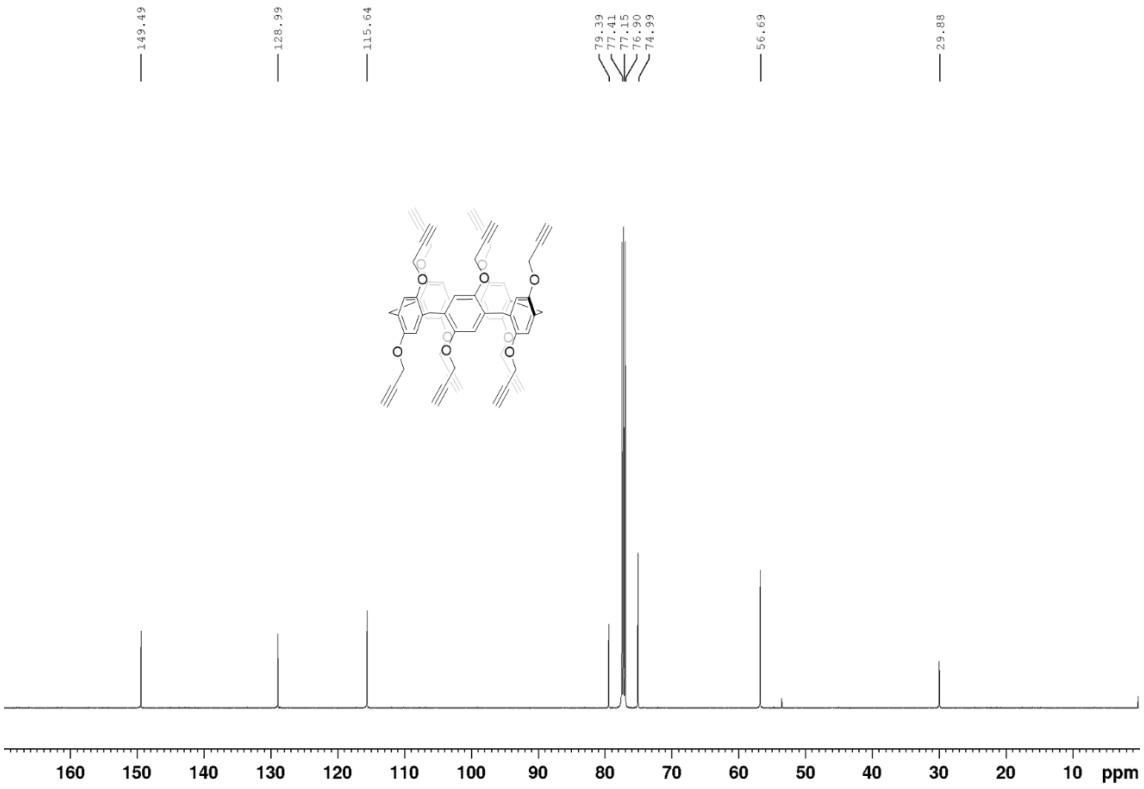

Figure S27. ^{13}C-NMR spectrum (100 MHz, 298K) of **9** in $CDCl_3$.

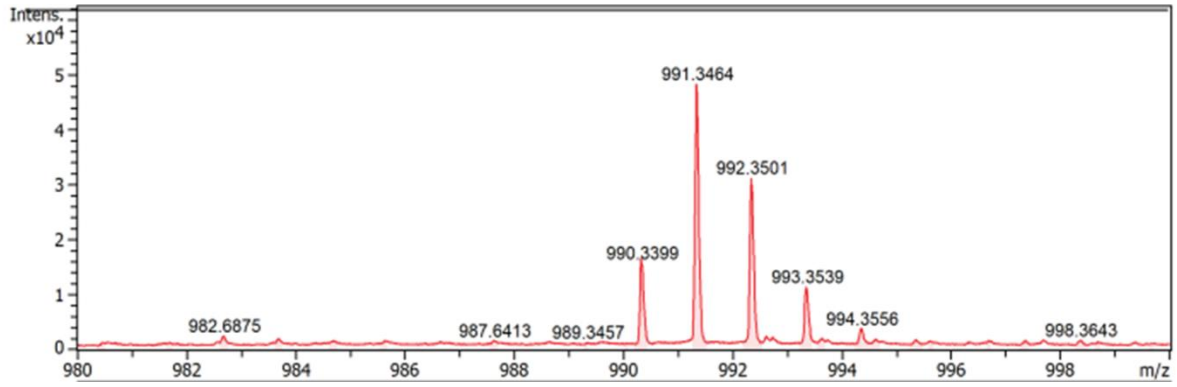

Figure S28. ESI-HRMS spectrum of **9** in CH_2Cl_2.

*1.3.3 Synthesis of acetyl mannose-substituted pillar[5]arene (**10**)*

Compound **9** (0.099 g, 0.010 mmol), compound **7** (0.1460 g, 0.30 mmol), and CuI (0.003 g, 0.018 mmol) were dissolved in THF (5 mL), and the mixture was stirred overnight at 60 ºC. The reaction mixture was poured into water and washed with CH_2Cl_2 three times. The organic layer was dried with Na_2SO_4. After removing the solvent, the crude product was purified by silica gel column chromatography, eluting with 5% MeOH in CH_2Cl_2, to obtain compound **10** as a pale-yellow solid (0.1300 g, 0.097 mmol, 92%). **^{1}H-NMR** (400 MHz, $CDCl_3$, ppm): δ = 7.91 (s, 10H; $CH_{triazole}$), 6.86 (d, 10H; $CH_{aromatic}$), 5.31–5.13 (m, 30H; CH), 4.91–4.86 (m, 20H; CH_2), 4.81–4.77 (m, 10H; CH), 4.60–4.59 (m, 20H, CH_2) 4.25–3.89 (m, 20H; CH_2), 3.83–3.68 (m, 20H; CH_2), 3.43–3.38 (m, 20H; CH_2) 2.05–1.89 (m, 120H; CH_3). **^{13}C-NMR** (100 MHz, $CDCl_3$, ppm): δ = 170.8 (C=O), 170.2 (C=O), 170.1 (C=O), 169.9 (C=O), 149.8 (ArC–O), 144.4 (C–N), 129.9, (ArC), 124.4 (C=CN), 97.9 (O-C-O), 69.5 (CH–O), 68.9 (CH–O), 66.5 (CH–O), 66.1 (CH–O), 65.9 (CH_2–O), 65.8 (CH_2–O), 62.6 (CH_2–O), 50.5 (CH_2–N), 21.0 (CH_3), 20.9 (CH_3), 20.9 (CH_3), 20.8 (CH_3). **MALDI-TOF** *m/z*: calcd. for $C_{225}H_{281}N_{30}O_{110}$ $[M]^+$, 5164.738; found 5164.815.

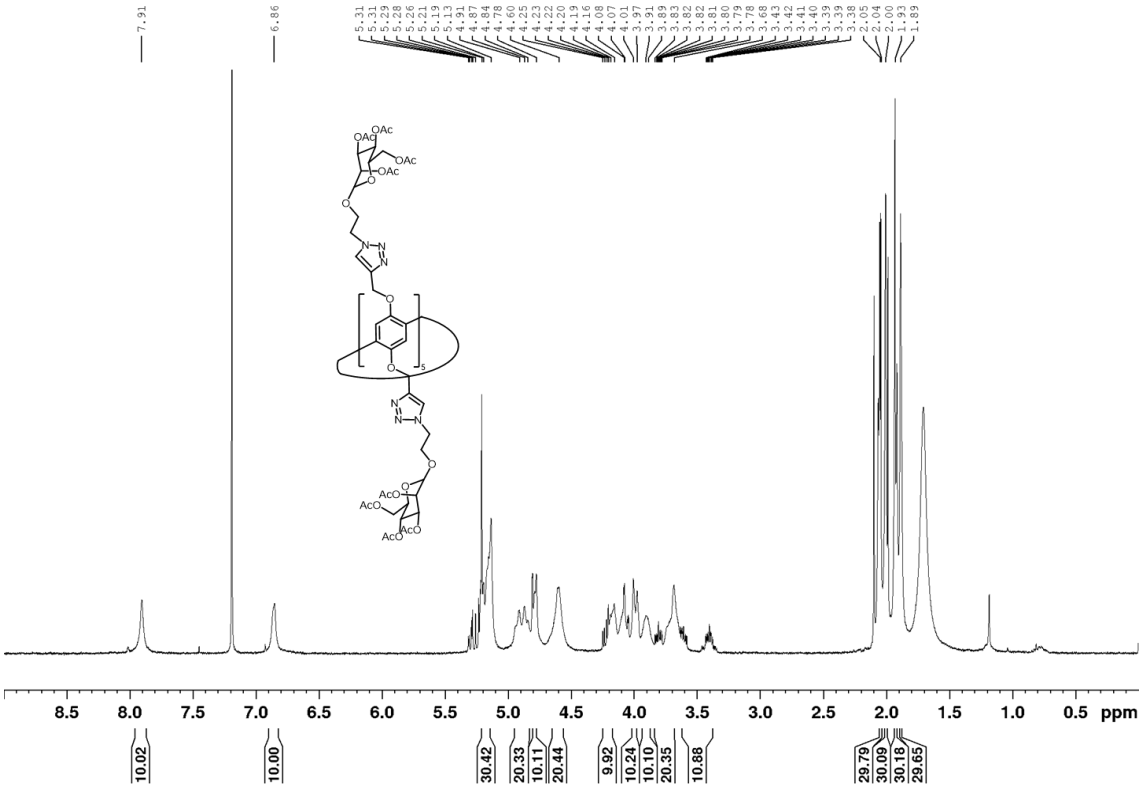

Figure S29. ^{1}H-NMR spectrum (400 MHz, 298K) of **10** in $CDCl_3$.

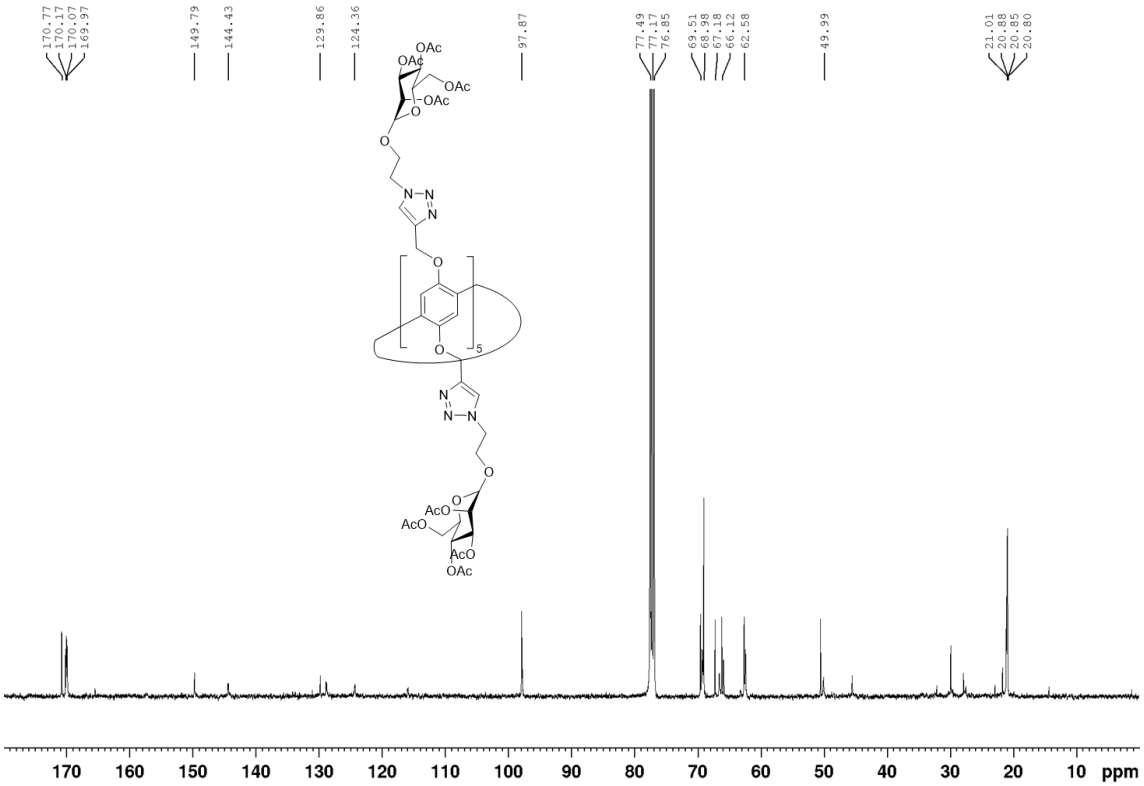

Figure S30. ^{13}C-NMR spectrum (100 MHz, 298K) of **10** in $CDCl_3$.

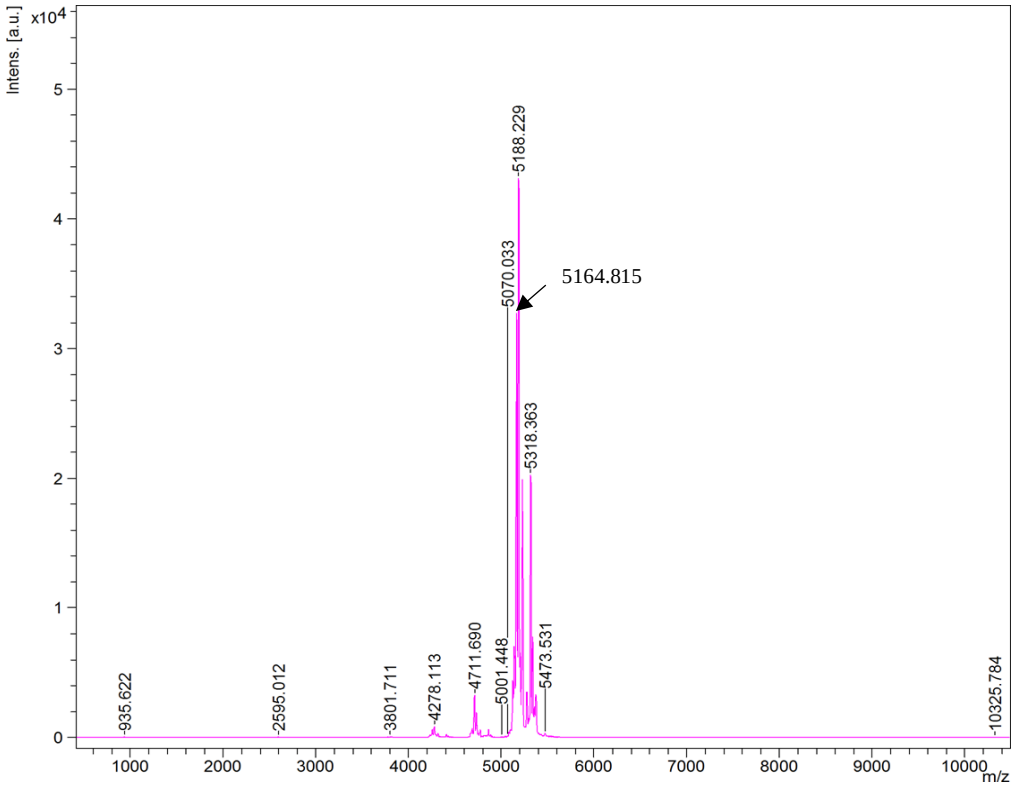

Figure S31. MALDI-TOF mass spectrum of **10**.

*1.3.4 Synthesis of a mannosylated pillar[5]arene (**WP5**)*

Compound **10** (0.13 g, 0.09 mmol) was dissolved in MeOH (5 mL). A solution of 1 M NaOMe in MeOH was added dropwise until the pH value reached 11. The reaction mixture was stirred at room temperature for 12 h. After the removal of the solvent, 10 mL water was added. The resulting aqueous solution was neutralized using Amberlite IR 120 H^+ resin, filtered, and washed three times with water. The obtained filtrate was concentrated to afford pure **WP5** as a yellow solid (0.10 g, 0.08 mmol, 87%). **^{1}H-NMR** (400 MHz, DMSO-d_6, ppm): δ = 8.24 (s, 10H, N–CH=C) triazole), 6.98 (s, 10H; $CH_{aromatic}$), 5.09 (d, 10H; CH), 4.80–4.76 (m, 10H; CH), 4.73–4.68 (m, 10H; CH), 4.63–4.59 (m, 20H; CH_2), 4.58–4.55 (m, 20H; CH_2), 4.50–4.45 (m, 10H; CH), 3.95–3.92 (m, 10H; CH), 3.79–3.75 (m, 10H; CH), 3.68–3.62 (m, 10H; CH), 3.56 (s, 10H; CH_2), 3.47–3.39 (m, 20H; CH_2). **^{13}C-NMR** (100 MHz, DMSO-d_6, ppm): δ= 148.8, 143.3, 128.2, 124.3, 114.4, 99.9, 74.1, 70.8, 70.1, 68.9, 65.6, 64.8, 61.1, 49.9, 49.3. **MALDI-TOF** *m/z*: calcd. for $C_{145}H_{200}N_{30}O_{70}$ $[M]^+$, 3484.343; found, 3484.301.

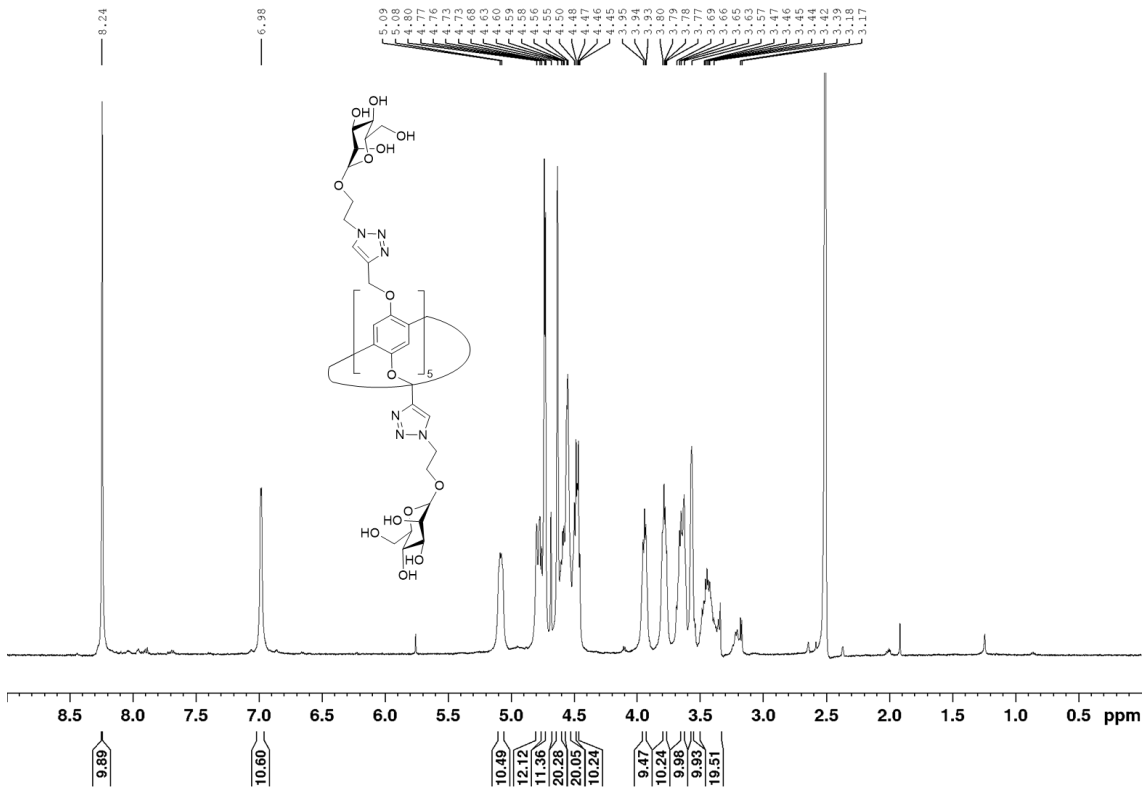

Figure S32. [1]H-NMR spectrum (400 MHz, 298K) of **WP5** in DMSO-d_6.

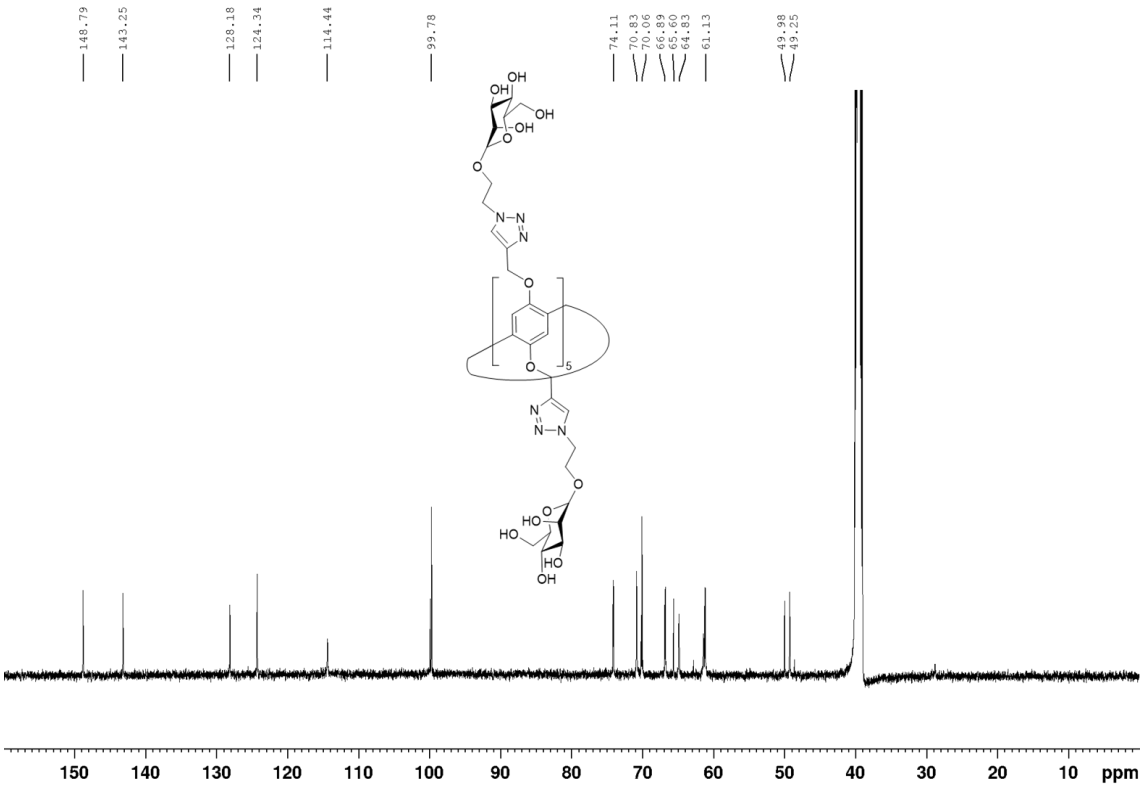

Figure S33. [13]C-NMR spectrum (100 MHz, 298K) of **WP5** in DMSO-d_6.

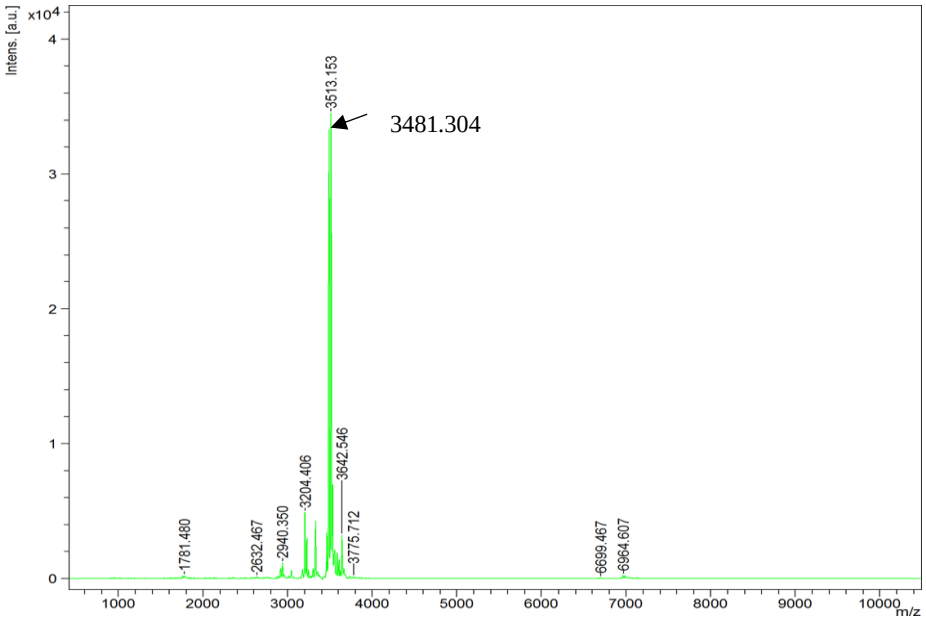

Figure S34. MALDI-TOF mass spectrum of **WP5**.

2. Preparation and characterization of PS3⊂WP5

2.1 Preparation of PS3⊂WP5

Each solution of **PS3** (0.66 mg, 0.0006 mmol) and **WP5** (2.09 mg, 0.0006 mmol) was first prepared in 1 mL dry THF. The **WP5** solution was then slowly added into 3 mL of DI water, followed by the addition of the **PS3** solution. The mixture was ultrasonicated for 10 min at room temperature. THF was removed by rotary evaporation, yielding the **PS3⊂WP5** complex in DI water. The resulting complex was characterized using UV-visible spectrophotometry, fluorescence spectrophotometry, transmission electron microscopy (TEM), dynamic light scattering (DLS), and zeta potential measurements.

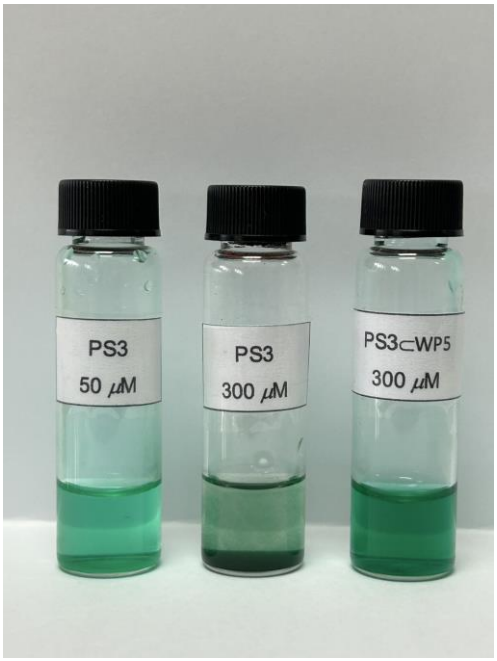

Figure S35. Photographs of aqueous dispersions of **PS3** and **PS3⊂WP5** under ambient conditions, highlighting differences in solubility.

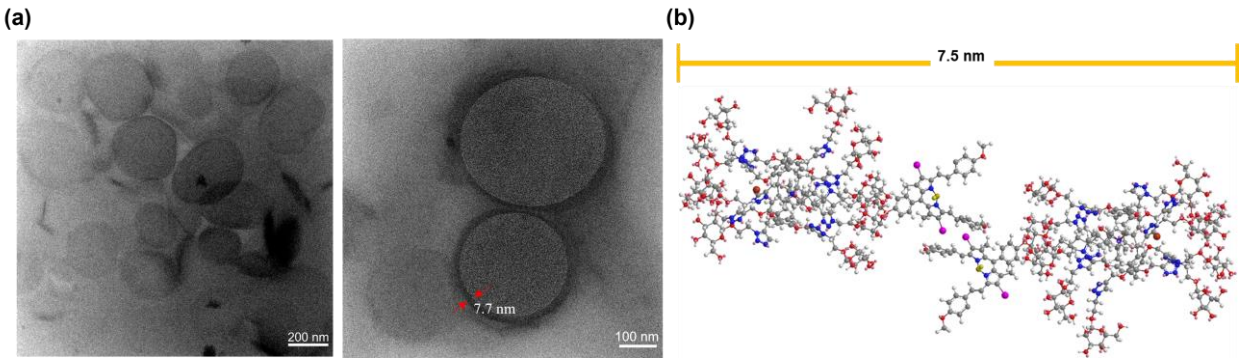

Figure S36. (a) TEM images of **PS3⊂WP5** self-assemblies showing multiple spherical particles with uniform morphology. A high-magnification image reveals a distinct shell structure with a membrane thickness around 7.7 nm. **(b)** Energy-minimized structure of **PS3⊂WP5** obtained from Chem3D calculations using the MM2 method.

2.2 UV-visible and fluorescence spectra

To prepare solutions for spectroscopic analysis, a stock solution of **PS3** (1×10^{-4} M) was prepared in dioxane and then diluted to 1×10^{-5} M in various solvents. Similarly, a stock solution of **PS3⊂WP5** (1×10^{-4} M) was prepared in water and diluted to 1×10^{-5} M in aqueous solutions. The absorption spectra were measured using a UV-vis spectrophotometer, and the emission spectra were recorded using a fluorescence spectrophotometer.

Table S1. Photophysical properties of **PS3** and **PS3⊂WP5** in various solvents.

PS	Solvent	$\lambda_{max,\ abs}$ **(nm)**	$\lambda_{max,\ em}$ **(nm)**	Stroke shift **(Δλ, nm)**	ε **(L·mol^{-1}·cm^{-1})**
PS3	H_2O	713	735	22	8600
	1:1 DMSO/H_2O	661	736	75	11500
	0.5% DMSO in H_2O	692, 730	736	6	18500 at 730
	DMSO	663	688	25	36600
	Toluene	668	681	13	5000
	CH_2Cl_2	660	678	18	14800
	EtOH	660	681	21	45400
	$CHCl_3$	662	682	20	54200
	EtOAc	658	672	14	6000
	Dioxane	660	676	16	5800
PS3⊂WP5	H_2O	730	737	7	18750
	1:1 DMSO/H_2O	726	737	11	12000
	0.5% DMSO in H_2O	730	737	7	19000
	DMSO	724	-	-	-
	EtOH	660, 730	-	-	50000 at 730 nm
	Dioxane	660	-	-	-
	CH_3CN	653	-	-	-
	THF	659	-	-	-

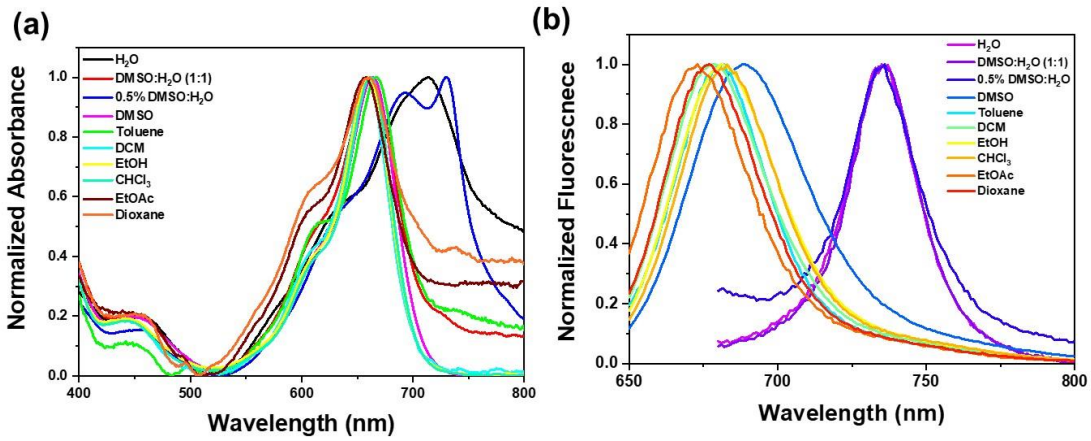

Figure S37. Normalized (a) absorbance and (b) emission spectra of **PS3** in various solvents.

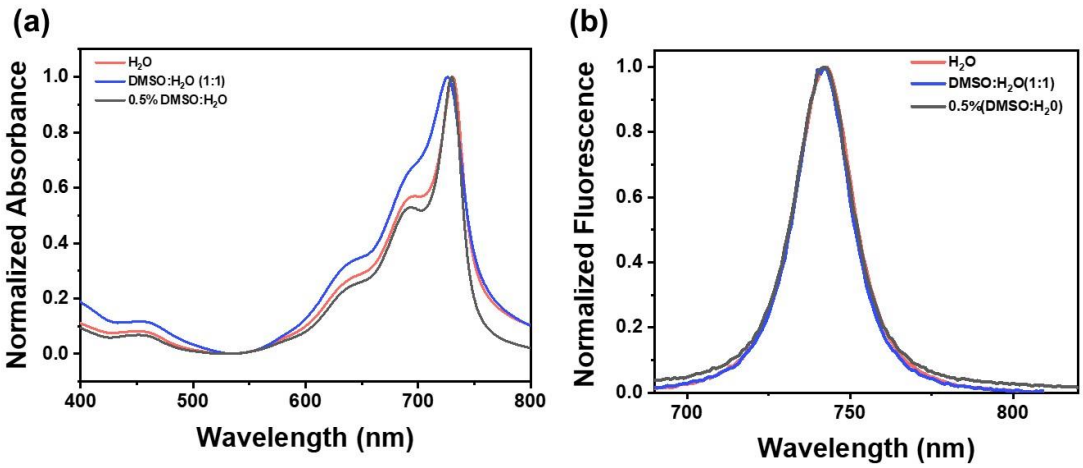

Figure S38. Normalized (a) absorbance and (b) emission spectra of **PS3⊂WP5** in aqueous solutions.

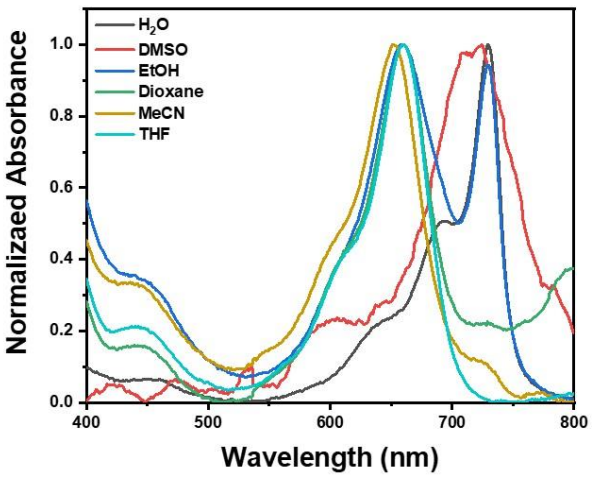

Figure S39. Normalized absorbance spectra of **PS3⊂WP5** in various organic solvents.

2.3 Fluorescence titration

A solution of the host **WP5** (10 µM) was prepared in DI water, and the guest **PS3** was gradually added at increasing concentration while keeping the concentration of **WP5** constant. The fluorescence emission spectra of **WP5** were recorded after each addition of **PS3**, using an excitation wavelength of 660 nm. The change in fluorescence intensity was monitored to assess the interaction between **WP5** and **PS3**. The fluorescence intensity increases with the addition of **PS3**, eventually reaching an equilibrium at a molar ratio of about 1:1, indicating the formation of a 1:1 host-guest complex. The red lines are linear fits used to determine the binding stoichiometry of the **PS3⊂WP5** complex.[5]

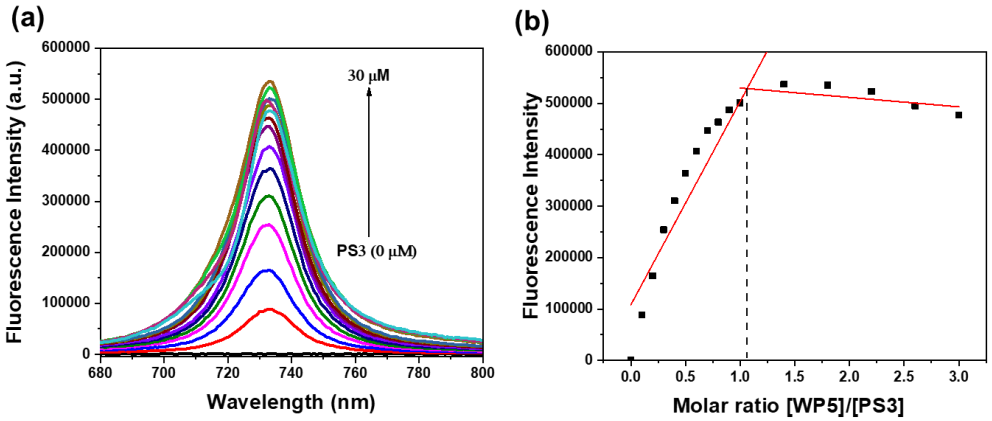

Figure S40. (a) Changes in the fluorescence spectra of **PS3** at concentrations ranging from 0 to 30 µM in the presence of 10 µM **WP5** in water. (b) Fluorescence titration curve of **WP5** (10 µM) with increasing concentrations of **PS3** (0–30 µM) in water.

2.4 Isothermal titration calorimetry (ITC)

Table S2. Summary of thermodynamic parameters related to the binding affinity and stability of the studied complex, including the number of binding sites (N site), dissociation constant (K_d), enthalpy change (ΔH), Gibbs free energy change (ΔG), and change in entropy ($-T\Delta S$).

Parameters	Value
N site	0.985 ± 0.03
K_d (M)	196×10^{-9}
ΔH (kJ·mol^{-1})	–14.7 ± 0.74
ΔG (kJ·mol^{-1})	–38.30
$-T\Delta S$ (kJ·mol^{-1})	–23.70

2.5 Dynamic light scattering (DLS)

To verify the stability of **PS3⊂WP5**, 200 µL of 3.5 µM **PS3⊂WP5** solution was added to each solution of 0.5 mL of phosphate-buffered saline (pH 7.4) and 0.5 mL of Eagle's Minimum Essential Medium (EMEM). The average particle size was then measured by DLS.

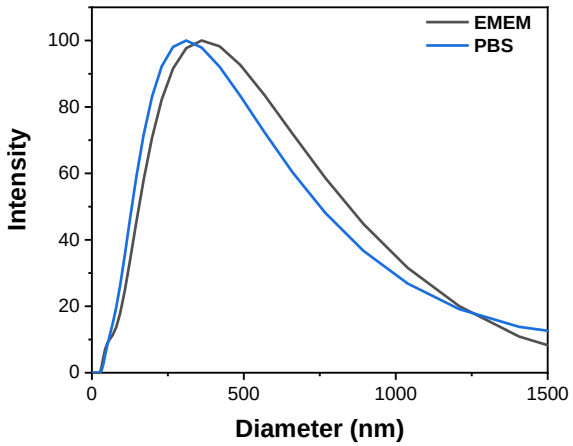

Figure S41. DLS data of **PS3⊂WP5** in EMEM and 1X PBS (pH = 7.4).

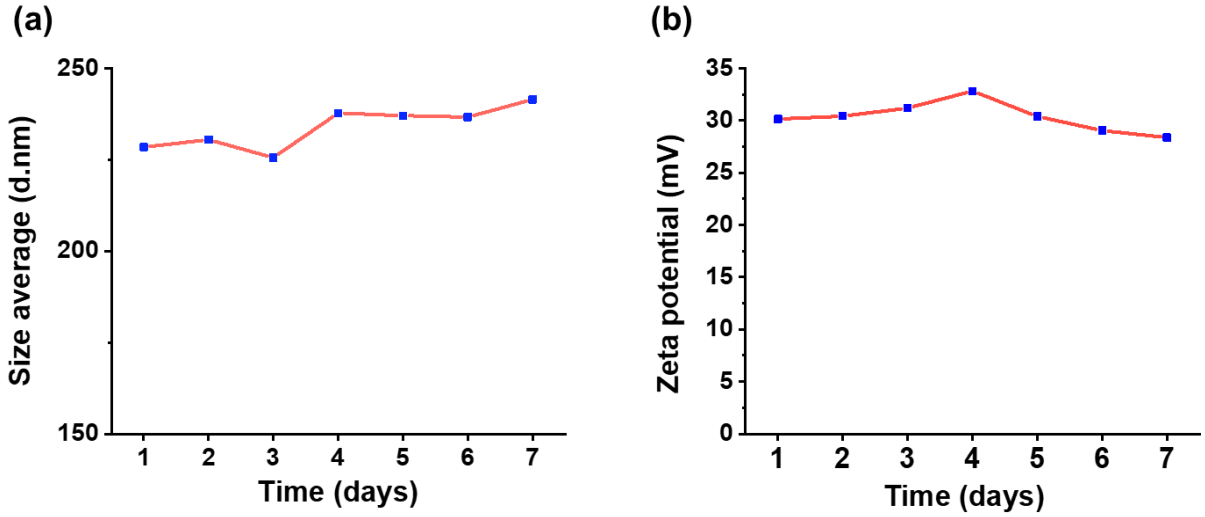

Figure S42. Time-course profiles of (a) hydrodynamic diameters and (b) zeta potentials of **PS3⊂WP5** nanoparticles monitored over 7 days in water at room temperature.

3. Evaluation of singlet oxygen quantum yield

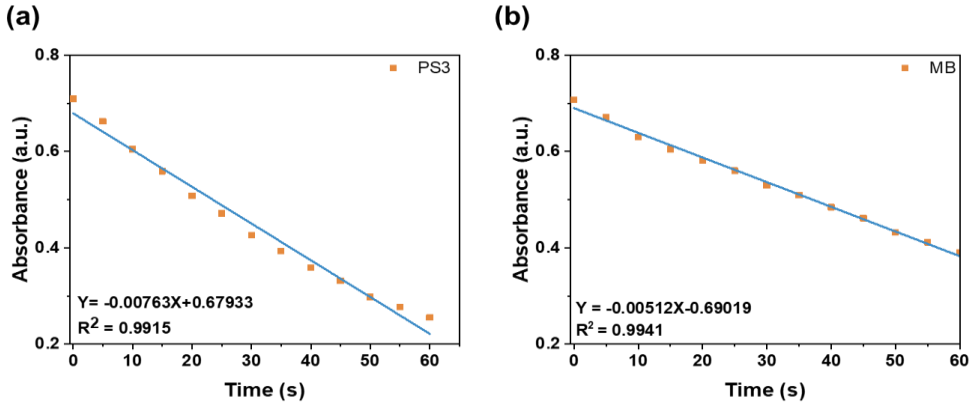

Figure S43. Linear fitting of DPBF decomposition with irradiation time in the presence of (a) 1.5 μM **PS3** and (b) 1.5 μM **MB** in CH_2Cl_2, showing the linear decrease in DPBF absorbance overtime.

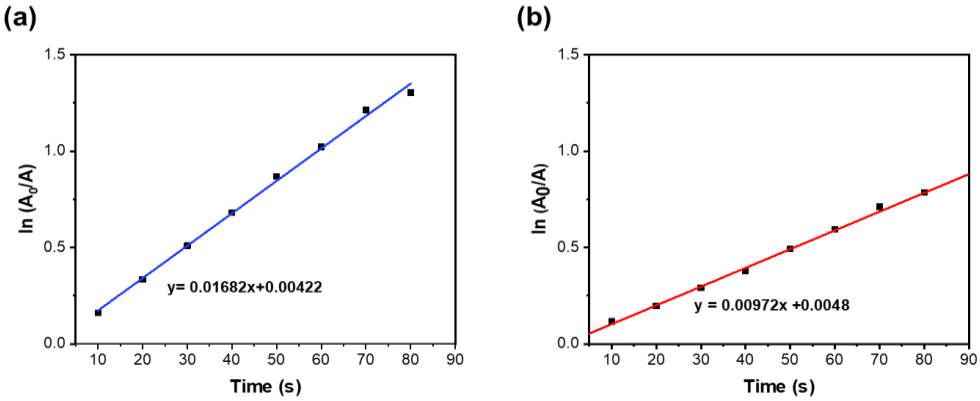

Figure S44. Time dependent decomposition of DPBF in CH_2Cl_2 by singlet oxygen produced by (a) **PS3** and (b) MB. A_0 represents the absorption of DPBF at 415 nm in the absence of irradiation whereas A is real-time absorption of DPBF at 415 nm at different irradiation time.

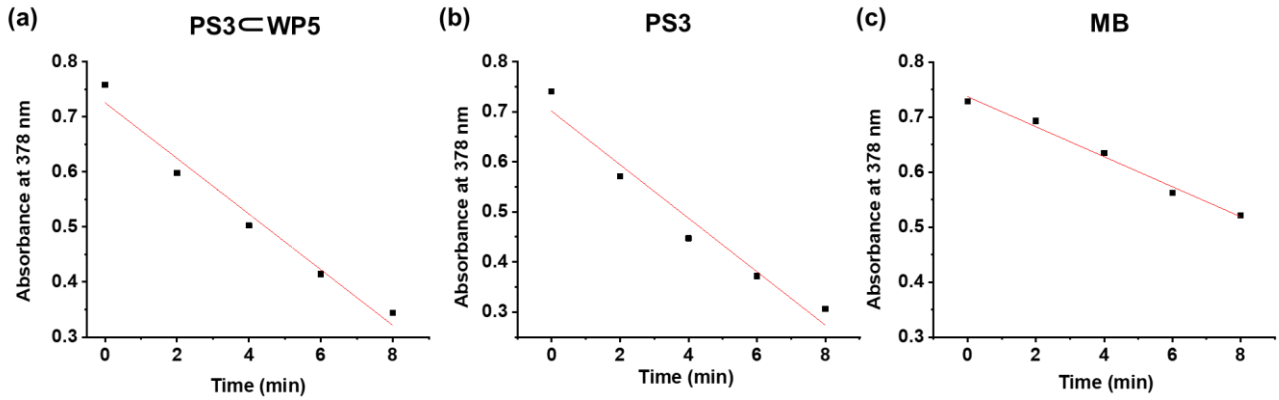

Figure S45. Linear fitting of ABDA decomposition over irradiation time in water in the presence of (a) 8 μM **PS3⊂WP5**, (b) 8 μM **PS3**, and (c) 8 μM MB, demonstrating the time-dependent linear decrease in ABDA absorbance, indicative of singlet oxygen generation.

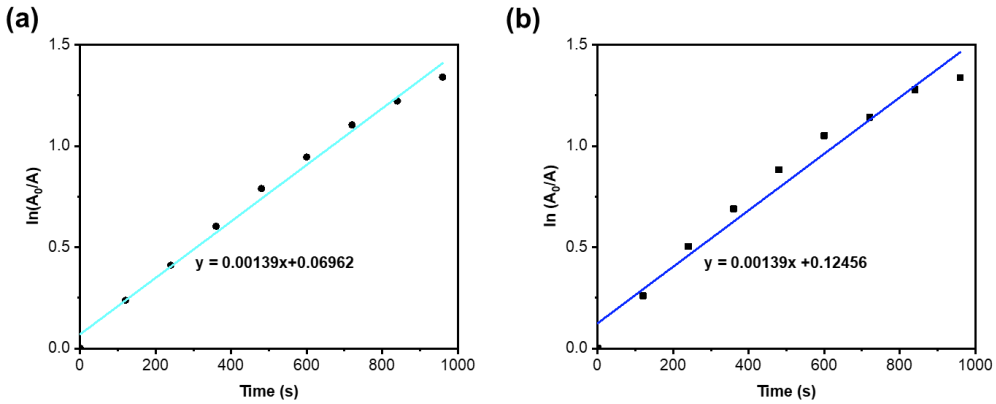

Figure S46. Time dependent decomposition of ABDA in water by singlet oxygen produced by (a) **PS3⊂WP5** and (b) **PS3**. A_0 represents the absorption of ABDA at 378 nm in the absence of irradiation whereas A is real-time absorption of ABDA at 378 nm at different irradiation time.

Table S3. Rate constant (k_{obs}) for the decay rate of ABDA and DPBF under various experimental conditions.

Photosensitizer	Trapping agent	Solvent	Observed rate constant (k_{obs}), s^{-1}
PS3	DPBF	CH_2Cl_2	16.8×10^{-2}
MB	DPBF	CH_2Cl_2	9.7×10^{-2}
PS3	ABDA	H_2O	1.4×10^{-4}
PS3⊂WP5	ABDA	H_2O	1.4×10^{-4}

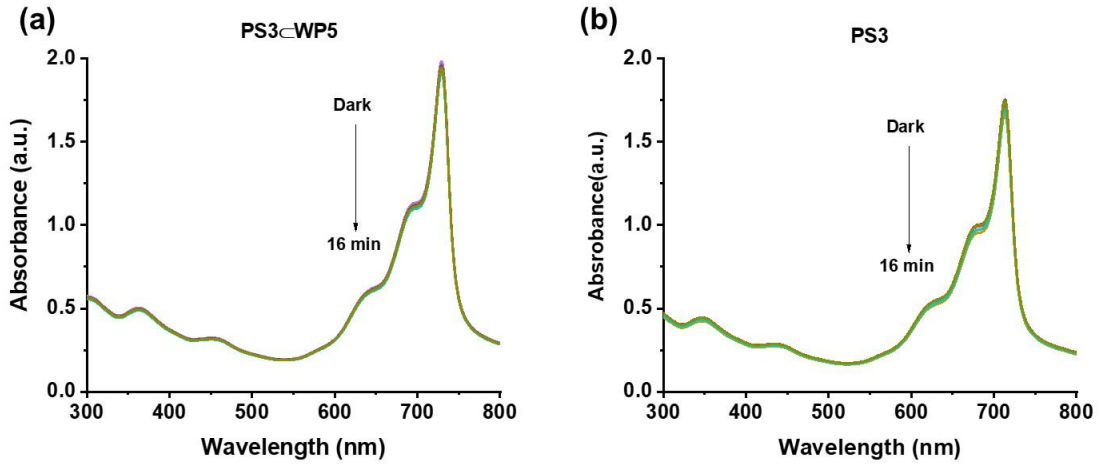

Figure S47. Photostability assessment of (a) **PS3⊂WP5** and (b) **PS3** in aqueous solutions under continuous light irradiation, monitored by UV-Vis absorption in the range of 300–800 nm.

4. Measurement of LED light wavelength

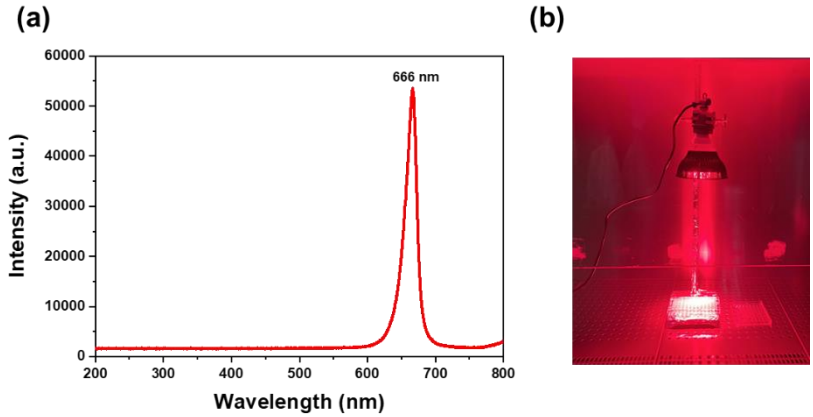

Figure S48. (a) Emission spectrum of the LED light source used to activate the **PS3⊂WP5** complex in *in vitro* phototoxicity experiments. (b) Photograph of the *in vitro* phototoxicity experimental setup.

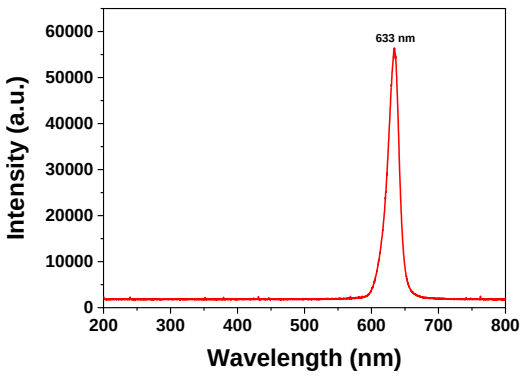

Figure S49. Emission spectrum of the LED light source used to activate **PS3** and the **PS3⊂WP5** complex in singlet oxygen generation experiments.

5. Cellular uptake of PS3 in MCF-7 breast cancer cells

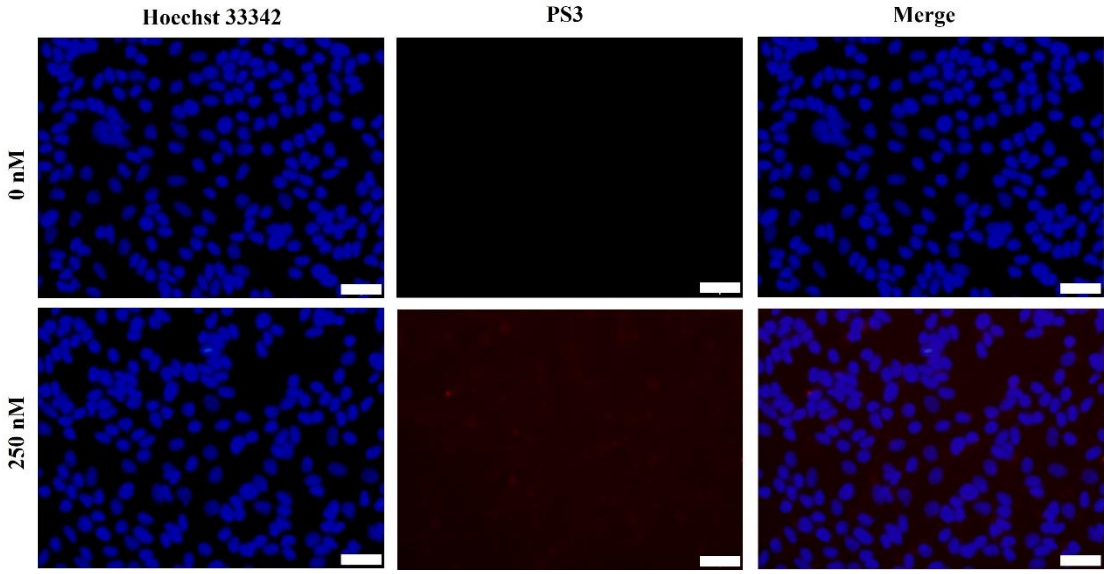

Figure S50. Immunofluorescence imaging of MCF-7 cells treated with 250 nM **PS3** for 24 h. Scale bar = 50 μm.

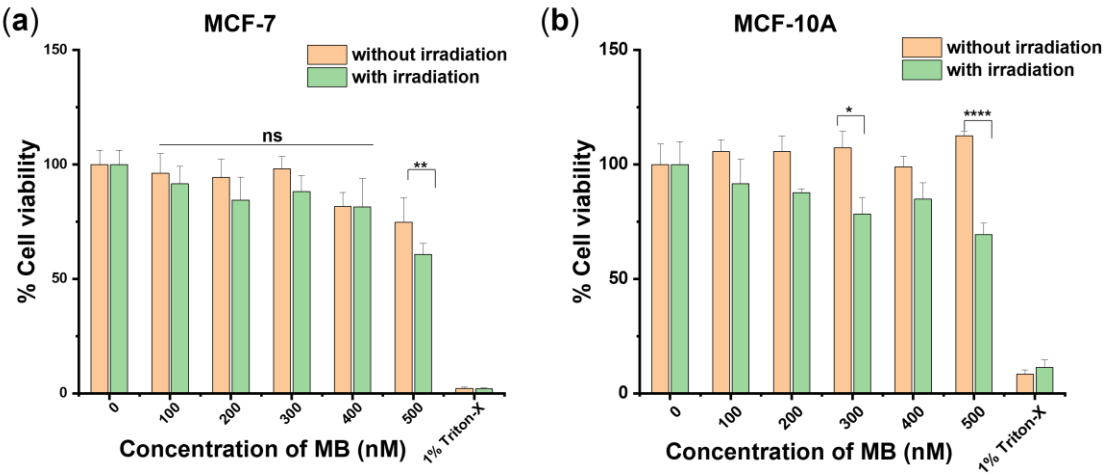

Figure S51. Cell viability of MCF-7 and MCF-10A cells after being treated with different concentrations of **MB** for 2 h, followed by exposure to the red-light LED lamp at a power of 45 mW/cm^2 for 30 min and further incubated in a humidified incubator for 24 h. The means ± SEM were obtained from triplications. The means ± SEM were obtained from three independent experiments, and statistical analysis was performed by two-way ANOVA, where ** $p < 0.01$, **** $p < 0.0001$, and ns = not significant.

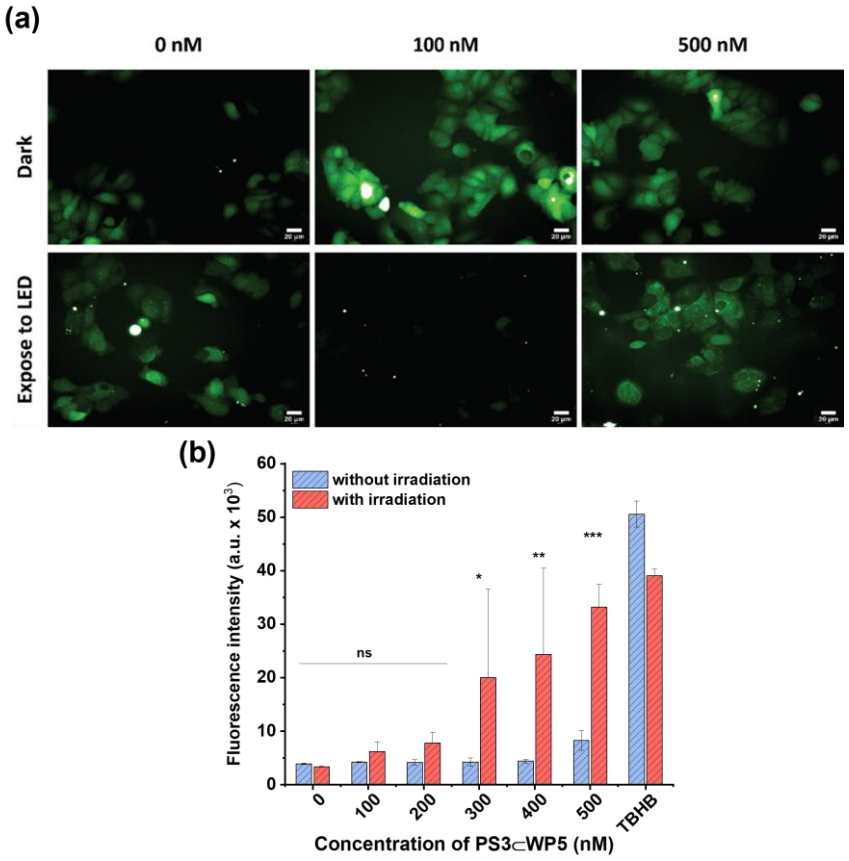

Figure S52. (a) The fluorescence image depicted the effect of 100 and 500 nM of **PS3⊂WP5** on ROS production in MCF-7 cells, both dark and exposed to the LED at 666 nm. ROS production is represented as green fluorescence. (b) ROS production was assessed using the DCFDA assay, by measuring fluorescence intensity (Ex/Em = 485/535 nm). TBHB was used as a positive control for ROS production. Effect of **PS3⊂WP5** concentrations on ROS production in MCF-7 cells was observed in the dark and upon exposure to LED red light for 30 min. The means ± SEM were obtained from triplications. The means ± SEM were obtained from three independent experiments, and statistical analysis was performed by two-way ANOVA where * $p < 0.1$, ** $p < 0.01$, *** $p < 0.001$, **** $p < 0.0001$, and ns = ns = not significant.

6. References

1) L.-B. Meng, W. Zhang, D. Li, Y. Li, X.-Y. Hu, L. Wang and G. Li, *Chem. Commun.*, 2015, **51**, 14381–14384.
2) J. Zou, Z. Yin, K. Ding, Q. Tang, J. Li, W. Si, J. Shao, Q. Zhang, W. Huang and X. Dong, *ACS Appl. Mater. Interfaces*, 2017, **9**, 32475–32481.
3) H. Charville, J. Jin, C. W. Evans, M. A. Brimble and D. E. Williams, *RSC Adv.*, 2013, **3**, 15435.
4) H. Deng, X. Shu, X. Hu, J. Li, X. Jia and C. Li, *Tetrahedron Lett.*, 2012, **53**, 4609–4612.
5) H. Duan, F. Cao, M. Zhang, M. Gao and L. Cao, *Chin. Chem. Lett.*, 2022, **33**, 2459–2463.